

# Time-Varying Sensor and Actuator Selection for Uncertain Cyber-Physical Systems

Ahmad F. Taha, *Member, IEEE*, Nikolaos Gatsis *Member, IEEE*, Tyler Summers *Member, IEEE*, Sebastian Nugroho, *Student Member, IEEE*.

**Abstract**—We propose methods to solve time-varying, sensor and actuator (SaA) selection problems for uncertain cyber-physical systems. We show that many SaA selection problems for optimizing a variety of control and estimation metrics can be posed as semidefinite optimization problems with mixed-integer bilinear matrix inequalities (MIBMIs). Although this class of optimization problems is computationally challenging, we present tractable approaches that directly tackle MIBMIs while providing both upper and lower bounds and lead to effective heuristics for SaA selection. The upper and lower bounds are obtained via successive convex approximations and semidefinite programming relaxations, respectively, and selections are obtained with a novel slicing algorithm from the solutions of the bounding problems. Custom branch-and-bound and combinatorial greedy approaches are also developed for a broad class of systems for comparison. Finally, comprehensive numerical experiments are performed to compare the different methods and illustrate their effectiveness.

**Index Terms**—Sensor and actuator selection, cyber-physical systems, linear matrix inequalities, controller design, observer design, greedy algorithms.

## I. INTRODUCTION & BRIEF LITERATURE REVIEW

**M**ANY emerging complex dynamical networks, from critical infrastructure to industrial cyber-physical systems (CPS) to various biological networks, are increasingly able to be instrumented with new sensing and actuation capabilities. These networks comprise growing webs of interconnected feedback loops and must operate efficiently and resiliently in dynamic and uncertain environments. The prospect of incorporating large numbers of additional sensors and actuators (SaAs) raises fundamental and important problems of jointly and dynamically selecting the most effective SaAs, in addition to simultaneously designing corresponding estimation and control laws associated with the selected SaAs.

There are many different quantitative notions of network controllability and observability that can be used as a basis for selecting effective SaAs in uncertain and dynamic cyber-physical networks. Notions based on classical Kalman rank conditions for linear systems focus on binary structural properties [1]–[5]. More elaborate quantitative notions based on Gramians [6]–[13] and classical optimal and robust control and estimation problems [14]–[20] for linear systems have also been studied. For selecting SaAs based on these metrics, several optimization methods are proposed in this literature,

including combinatorial greedy algorithms [9], [19], convex relaxation heuristics using sparsity-inducing  $\ell_1$  penalty functions [14]–[16] and branch-and-bound and Big-M techniques for mixed-integer semidefinite programming [13], [20].

Despite the recent surge of interest in quantifying network controllability and observability and in associated SaA selection problems, a much wider set of metrics are relevant for uncertain cyber-physical systems. The existing literature tends to focus mainly on classical metrics (e.g., involving Kalman rank, Gramians, Linear Quadratic Regulators, and Kalman Filters) and deterministic linear time invariant systems. Methods for time varying systems with various uncertainties, constraints, and nonlinearities are also important to broaden applicability. It is well known that a broad variety of systems and control problems can be cast in the form of semidefinite programs (SDP) and linear matrix inequalities (LMI) [21], but many of these more recent formulations have not been considered in the context of SaA selection. In general, the joint selection of SaAs and design of associated estimation and control laws for many metrics can be posed as semidefinite optimization problems with mixed-integer bilinear matrix inequalities (MIBMIs).

Here we propose methods to solve time-varying, sensor and actuator (SaA) selection problems for uncertain cyber-physical systems. Our methods can be applied to any of the broad range of problems formulated as MIBMIs. Although this class of optimization problems is computationally challenging, we present tractable approaches based directly on the MIBMIs that provide both upper and lower bounds and lead to effective heuristics for SaA selection. The upper and lower bounds are obtained via successive convex approximations and SDP relaxations, respectively, and selections are obtained with a novel slicing algorithm from the solutions of the bounding problems. The direct derivation of approximations and relaxations from the MIBMIs contrasts our approach with other existing convex optimization-based approaches. The time-varying aspect allows SaA selections to change dynamically based on time varying conditions in the network. Custom branch-and-bound and combinatorial greedy approaches are also developed for a broad class of systems for comparison. Finally, comprehensive numerical experiments are performed to compare the different methods and illustrate their effectiveness.

A preliminary version of this work appeared in [22] where we developed customized algorithms for actuator selection, and here we significantly extended the methodology with the successive convex approximation and convex relaxation approaches and provide much more extensive numerical experiments.

The next section presents the framework and problem formulation, and details the paper contributions and organization.

Ahmad F. Taha, Nikolaos Gatsis, and Sebastian Nugroho are affiliated with the Department of Electrical and Computer Engineering at the University of Texas San Antonio. Tyler Summers is with the Department of Mechanical Engineering, University of Texas at Dallas. Emails: {ahmad.taha, nikolaos.gatsis,sebastian.nugroho}@utsa.edu, tyler.summers@utdallas.edu. This material is based upon work supported in part by the National Science Foundation under Grants No. ECCS-1462404, CMMI 1728629, and CMMI 1728605. The work of T. Summers was partially sponsored by the Army Research Office and was partially accomplished under Grant Number: W911NF-17-1-0058.

## II. PROBLEM FORMULATION AND PAPER CONTRIBUTIONS

### A. Nonlinear and Uncertain CPS Model

The notation used in the paper is included in Appendix A. We consider a general class of dynamic CPSs modeled as

$$\dot{\mathbf{x}}(t) = \mathbf{A}\mathbf{x}(t) + \mathbf{B}_u\mathbf{u}(t) + \mathbf{B}_w\mathbf{w}(t) + \mathbf{B}_f\mathbf{f}(\mathbf{x}), \quad (1a)$$

$$\mathbf{y}(t) = \mathbf{C}\mathbf{x}(t) + \mathbf{D}_u\mathbf{u}(t) + \mathbf{D}_v\mathbf{v}(t), \quad \mathbf{x}(t_0) = \mathbf{x}_0 \quad (1b)$$

The network state  $\mathbf{x}(t) \in \mathbb{R}^{n_x}$  consists of each of  $N$  nodal agent states  $\mathbf{x}_i \in \mathbb{R}^{n_{x_i}}$ ,  $i = 1, \dots, N$ . The dynamics of the CPS nodes are coupled through the state-vector evolution (1). Likewise, each nodal agent has a set of available inputs  $\mathbf{u}_i \in \mathbb{R}^{n_{u_i}}$  and measurements  $\mathbf{y}_i(t) = \mathbf{C}_i\mathbf{x}(t) \in \mathbb{R}^{n_{y_i}}$ . The mapping from the input to state vector can thus be written in the form  $\mathbf{B}_u = \text{blkdiag}(\mathbf{B}_{u_1}, \dots, \mathbf{B}_{u_N})$ . The system nonlinearity can be expressed as  $\mathbf{f}(\mathbf{x}) \in \mathbb{R}^{n_x}$  and  $\mathbf{B}_f$  represents the distribution of the nonlinearities. In summary, the system has  $n_x$  states,  $n_u$  control inputs,  $n_y$  output measurements,  $n_w$  unknown inputs (UIs), and  $n_v$  data perturbations.

**Remark 1.** *The UIs account for a wide range of perturbations such as modeling errors, unknown parameters, noise, unmeasurable inputs, and actuator faults. The data perturbations incorporate measurement noise, bad data, and cyber-attacks (e.g., denial of service, replay, and data integrity attacks).*

### B. Problem Formulation

The objective of the methods presented in this paper is two-fold, namely, to model the time-varying SaA selection problem and to propose scalable methods to address this problem for uncertain CPSs following general dynamical models. To formally state the SaA selection problem, we define binary variables  $\pi_i$ ,  $i = 1, \dots, N$ , where  $\pi_i = 1$  if the actuator of the  $i$ -th nodal agent is selected, and 0 otherwise. Similarly, we define binary variables  $\gamma_i$ ,  $i = 1, \dots, N$ , where  $\gamma_i = 1$  if the sensor of the  $i$ -th nodal agent is selected, and 0 otherwise. Variables  $\pi_i$  and  $\gamma_i$  are organized in vectors  $\boldsymbol{\pi}$  and  $\boldsymbol{\gamma}$ . Given the definitions, the uncertain dynamics can be written as

$$\dot{\mathbf{x}}(t) = \mathbf{A}^j\mathbf{x}(t) + \mathbf{B}_u^j\boldsymbol{\Pi}^j\mathbf{u}(t) + \mathbf{B}_w^j\mathbf{w}(t) + \mathbf{B}_f^j\mathbf{f}^j(\mathbf{x}), \quad (2a)$$

$$\mathbf{y}(t) = \boldsymbol{\Gamma}^j\mathbf{C}^j\mathbf{x}(t) + \mathbf{D}_u^j\mathbf{u}(t) + \mathbf{D}_v^j\mathbf{v}(t), \quad \mathbf{x}^j(t_0) = \mathbf{x}_0^j \quad (2b)$$

where  $j$  denotes the time-period (see Remark 2);  $\boldsymbol{\Pi} = \text{blkdiag}(\pi_1\mathbf{I}_{n_{u_1}}, \dots, \pi_N\mathbf{I}_{n_{u_N}})$  places vector  $\boldsymbol{\pi}$  in a block diagonal matrix of appropriate dimensions (variables  $\boldsymbol{\Pi}$  and  $\boldsymbol{\pi}$  are thus used interchangeably), and likewise  $\boldsymbol{\Gamma} = \text{blkdiag}(\gamma_1\mathbf{I}_{n_{y_1}}, \dots, \gamma_N\mathbf{I}_{n_{y_N}})$ . Without loss of generality, we assume that the SaA selection problem entails activating sensors and actuators from individual subsystems, rather than picking what measurements or actuators that are selected from each system.

**Remark 2** (Topological Evolution). *In (2), the optimal SaA selection and the control/estimation laws change from one time-period to another. The time-frame depends on the application under study, and the state-space matrices are obtained through an a priori analysis of the system dynamics. For example, in power networks the state-space matrices ( $\mathbf{A}^j, \mathbf{B}_u^j, \dots$ ) change according to the operating point of the*

*system which is determined via optimal power flow routines. The time-horizon of this change is around 5 minutes. In water distribution networks, this change is often in hours as the water demand patterns and water flows evolve at a slower time-scale than electric power demand [23].*

The high-level problem for time-varying SaA selection can be formulated as follows:

$$\min \sum_{j=1}^{T_f} \{c_{\pi,j}(\boldsymbol{\pi}^j) + c_{\gamma,j}(\boldsymbol{\gamma}^j) + \text{CtrlObj} + \text{EstObj}\} \quad (3a)$$

$$\text{subject to (2), } \{\boldsymbol{\pi}^j\}_{j=1}^{T_f} \in \mathcal{P}, \{\boldsymbol{\gamma}^j\}_{j=1}^{T_f} \in \mathcal{G} \quad (3b)$$

$$\text{CtrlConstraints}(\boldsymbol{\pi}^j), \text{EstConstraints}(\boldsymbol{\gamma}^j). \quad (3c)$$

In (3), the objective is to minimize the sum of the cost as a function of the selected SaAs and certain control and estimation metrics, which are described in the next section. The constraints include the dynamical system evolution for all time-periods  $j \in \{1, \dots, T_f\}$ , and operational set constrains ( $\mathcal{P}$  and  $\mathcal{G}$ ) on  $\boldsymbol{\gamma}$  and  $\boldsymbol{\pi}$  that include the binary nature of these variables and possibly *ramp constraints* as a function of previous SaA selection. The control and estimation constraints depend on the considered estimation and control metrics which can be written as SDPs in many cases as discussed in the next section.

### C. Paper Organization and Contributions

The common instrument we use in this paper is SDPs. The formulations in this paper are building on semidefinite programming approaches for robust control and estimation routines, since SDP-based methods and solvers have become common and efficient over the past 20 years. The reader is referred to [21] and [24] for many SDP formulations for optimal control and estimation methods.

**Disclaimer:** Although there are many polynomial-time algorithms to solve SDPs, many existing implementations do not scale graciously with the number of states and control inputs. However, recent advancements in quantum semidefinite programming solvers that use a combination of polynomial speedups, quantum annealing, and machine learning promise significant improvements in terms of the worst case complexity [25], [26]. In addition, recent techniques that solve an iterative sequence of linear programs or second order cone programs are capable of providing good approximations of SDP solutions [27], and hence more tractable than general-purpose SDP solvers. Furthermore, more efficient SDP solver implementations in Julia [28, Table I] show major improvements over implementations in CVX or Yalmip. Finally, and given state-space parameters ahead of time, SDPs as the ones presented in this paper can be solved offline.

To set the stage, we first succinctly list control and estimation formulations as SDPs in Tables VII and VIII in Appendix E, where the system dynamics, controller/observer form, optimization variables, and the optimization problem are stated. The listed formulations are instrumental in formalizing the SaA selection problem since the LMIs share a similar structure. Many other control and estimation laws

can fit directly into the proposed methodologies. The main contributions of this paper are detailed next.

- First, we show that a large array of optimal control and estimation problems with SaA selection share a similar level of computational complexity of solving optimization problems with MIBMIs (Section III).
- Second, we develop one-shot convex relaxation that produces a lower bound to the original problem with MIBMIs. Two successive convex approximations that yield upper bounds are also developed. (Sections IV–VI).
- Third, theoretical guarantees on the convergence of the convex relaxations and approximations are provided, with the necessary background and assumptions.
- Fourth, we develop simple algorithms to recover the binary selection of SaAs, in addition to the state-feedback gains and performance indices (Appendix D).
- Fifth, we include a general formulation that utilizes the Big-M method [29], thereby transforming the optimization problem from MIBMIs to a mixed-integer semidefinite program (MISDP); see Section VII.
- Sixth, we present as an alternative a suboptimal, greedy algorithm to solve the combinatorial SaA selection problem in Section VIII.
- Finally, comprehensive numerical examples are provided in Section IX. The results show the performance of the developed methods and that the optimal solution to the relaxed MIBMIs is nearly obtained in mostly all instances of our study. The numerical results also corroborate the theoretical results, and the necessary assumptions needed to obtain convergence are satisfied.

The next section presents the developed framework of time-varying SaA selection for uncertain dynamic systems.

### III. TIME-VARYING SAA SELECTION WITH VARIOUS METRICS: A UNIFYING MIBMI FRAMEWORK

In this section, we show that a plethora of control or estimation problems with time-varying SaA can be written as nonconvex optimization problems with MIBMIs. This observation considers different formulations pertaining to various observability and controllability metrics.

In particular, replacing  $B_u$  with  $B_u\Pi$  and  $C$  with  $\Gamma C$  in the SDPs in Tables VII and VIII significantly increases the complexity of the optimization problem. This transforms the SDPs into nonconvex problems with MIBMIs, thereby necessitating the development of advanced optimization algorithms—the major contribution of this paper. For compactness, we only consider the actuator selection problem for robust  $\mathcal{L}_\infty$  control of uncertain linear systems (see the second row of Table VII or [30]), and leave the other problems as simple extensions. Under this simplifying setup, the system dynamics can be written as:

$$\dot{\mathbf{x}}(t) = \mathbf{A}^j \mathbf{x}(t) + \mathbf{B}_u^j \Pi^j \mathbf{u}(t) + \mathbf{B}_w^j \mathbf{w}(t) \quad (4a)$$

$$z(t) = \mathbf{C}_z^j \mathbf{x}(t) + \mathbf{D}_{wz}^j \mathbf{w}(t) \quad (4b)$$

where  $\Pi^j$  is binary matrix variable (cf. Section II) and  $z(t)$  is the control performance index. The time varying sequence of

selected actuators and stabilizing controllers is obtained as the solution of the following multi-period optimization problem:

$$\underset{\{\mathbf{S}, \mathbf{Z}, \zeta, \boldsymbol{\pi}\}^j}{\text{minimize}} \quad \sum_{j=1}^{T_f} \zeta^j + \alpha_\pi^\top \boldsymbol{\pi}^j \quad (5a)$$

$$\text{subject to} \quad \begin{bmatrix} \mathbf{A}^j \mathbf{S}^j + \mathbf{S}^j \mathbf{A}^{j\top} + 2\alpha \mathbf{S}^j & & \\ -\mathbf{B}_u^j \Pi^j \mathbf{Z}^j - \mathbf{Z}^{j\top} \Pi^j \mathbf{B}_u^{j\top} & \mathbf{B}_w^j & \\ & \mathbf{B}_w^{j\top} & -2\alpha \mathbf{I} \end{bmatrix} \preceq \mathbf{O} \quad (5b)$$

$$\begin{bmatrix} -\mathbf{S}^j & \mathbf{O} & \mathbf{S}^j \mathbf{C}_z^{j\top} \\ \mathbf{O} & -\mathbf{I} & \mathbf{D}_{wz}^{\top} \\ \mathbf{C}_z^j \mathbf{S}^j & \mathbf{D}_{wz}^j & -\zeta^j \mathbf{I} \end{bmatrix} \succeq \mathbf{O} \quad (5c)$$

$$\mathbf{H} \boldsymbol{\pi} \leq \mathbf{h}, \quad \boldsymbol{\pi} \in \{0, 1\}^N. \quad (5d)$$

In (5), the optimization variables are matrices  $(\mathbf{S}, \mathbf{Z}, \mathbf{Y})^j$ , the actuator selection  $\boldsymbol{\pi}^j$  (collected in vector  $\boldsymbol{\pi}$  for all  $j$ ), and the robust control index  $\zeta^j$  for all  $j \in \{1, \dots, T_f\}$ . Given the solution to (5), the stabilizing control law for the  $\mathcal{L}_\infty$  problem can be written as  $\mathbf{u}^*(t) = -\mathbf{Z}^{*j} (\mathbf{S}^{*j})^{-1} \mathbf{x}(t)$  for all  $t \in [t_j, t_{j+1})$ . This guarantees that  $\|\mathbf{z}\| \leq \sqrt{\mu^*} \|\mathbf{w}\|$ . The logistic constraint  $\mathbf{H} \boldsymbol{\pi} \leq \mathbf{h}$  couples the selected actuators across time periods, and is discussed in Appendix B.

The optimization problem (5) includes MIBMIs due to the term  $\mathbf{B}_u^j \Pi^j \mathbf{Z}^j$ . The bilinearity together with the integrality constraints bring about the need for specialized optimization methods. It should be emphasized that (5) is *not* a mixed-integer convex program. Therefore, general-purpose mixed-integer convex programming solvers are not applicable. Interestingly, the design of the remaining controllers and observers in Tables VII and VIII largely share the optimization complexity of problem (5). It can be easily observed that *all* design problems in the two tables feature MIBMIs with the form  $\mathbf{B}_u \Pi \mathbf{Z} + \mathbf{Z}^\top \Pi \mathbf{B}_u^\top$  or a similar one. This simple idea signifies the impact of finding a solution to optimization problems with MIBMIs. In fact, the LMI formulations for control problems in [21] and other studies become MIBMIs when SaA selection is included. Using (5) as an exemplification for other problems with similar non-convexities, custom optimization algorithms to deal with such MIBMIs are proposed in the ensuing sections.

**Remark 3** (Common or Piecewise Quadratic Lyapunov Functions). *The proposed formulation does not take into account obtaining a common Lyapunov function between all time-periods for two reasons: (1) By construction, we assume that the topological evolution or the change in the state-space matrices is not faster than the time it takes the system to reach steady-state. Hence, the final state value for time-period  $j$  is assumed to be the initial value for time-period  $j + 1$ . (2) The existence of common quadratic Lyapunov function is often a very conservative sufficiency condition [31], especially in large-scale systems.*

As an alternative to obtaining a common Lyapunov function, LMIs for piecewise quadratic Lyapunov functions can be formulated [31]. In particular, instead of finding a common  $\mathbf{S}$  for LMIs  $\mathbf{S} \mathbf{A}^{j\top} + \mathbf{A}^j \mathbf{S} \prec \mathbf{O}$ ,  $j = 1, \dots, T_f$ , this stringent condition can be relaxed by obtaining different  $\mathbf{S}_j$ 's, while adding other LMIs that make the Lyapunov function piecewise





$$\begin{aligned}
&= \text{trace} \left( \mathbf{E} \mathbf{v}_{i,(l,m)} \mathbf{v}_{i,(l,m)}^\top \right) \\
&= \text{trace} \left( \mathbf{E} \mathbf{V}_{i,(l,m)} \right) \quad (20)
\end{aligned}$$

The previous development reveals that constraint (14) is equivalent to the constraint  $\text{trace}(\mathbf{E} \mathbf{V}_{i,(l,m)}) - \mathbf{e}^\top \mathbf{v}_{i,(l,m)} = 0$ , which is linear in  $\mathbf{V}_{i,(l,m)}$  and  $\mathbf{v}_{i,(l,m)}$ , as long as the constraint  $\mathbf{V}_{i,(l,m)} = \mathbf{v}_{i,(l,m)} \mathbf{v}_{i,(l,m)}^\top$  is imposed, which is nonconvex. The constraint  $\mathbf{V}_{i,(l,m)} = \mathbf{v}_{i,(l,m)} \mathbf{v}_{i,(l,m)}^\top$  is equivalent to

$$\begin{bmatrix} \mathbf{V}_{i,(l,m)} & \mathbf{v}_{i,(l,m)} \\ \mathbf{v}_{i,(l,m)}^\top & 1 \end{bmatrix} \succeq \mathbf{O}, \quad \text{rank}(\mathbf{V}_{i,(l,m)}) = 1. \quad (21)$$

The rank constraint above is nonconvex, and by dropping it, we obtain the convex relaxation (17) of (15). As a relaxation of (15), its optimal value has the property that  $\tilde{L} \leq L$ . ■

Proposition 2 asserts that  $\tilde{L} = L$  if  $\text{rank}[\mathbf{V}_{i,(l,m)}] = 1$ . Since the rank constraint is nonconvex, it is reasonable to consider surrogates for the rank in an effort to make the relaxation (17) tighter; one such surrogate is the nuclear norm of a matrix [34]. Thus, the constraint  $\|\mathbf{V}_{i,(l,m)}\|_* \leq 1$  can be added to promote smaller rank for  $\mathbf{V}_{i,(l,m)}$ ; the optimal value of (17) is impacted as follows.

**Corollary 1.** *Let  $\tilde{L}$  be the optimal value of (17) with the added constraint  $\|\mathbf{V}_{i,(l,m)}\|_* \leq 1$ . It holds that  $\tilde{L} \geq \tilde{L}$ .*

*Proof of Corollary 1:* Adding the constraint restricts the feasible set of (17), yielding the stated relationship between the optimal values. ■

## VI. CONVEX APPROXIMATIONS: AN UPPER BOUND ON (8)

The common thread between the previous and the present section is to replace the nonconvex feasible set given by constraints (6b), (6c), (6d), and (7) with convex sets. While the previous section relies on convex relaxations of the nonconvex feasible set, this section develops convex restrictions, i.e., replaces the nonconvex feasible set with a convex subset. The premise is to solve a series of optimization problems, in which the convex subset is improved. Thus, the algorithms in this section fall under the class of *successive convex approximations* (SCAs). Two SCA algorithms are developed in this section. Due to the convex restriction, the algorithms solve optimization problems that yield upper bounds for the optimal value  $L$  of problem (8).

Because the SCA algorithms rely on forming convex subsets of the feasible nonconvex set, they must be initialized at interior points of the nonconvex feasible set. The next proposition asserts that such points indeed exist under Assumption 1.

**Proposition 3.** *Under Assumption 1, problem (8) is strictly feasible, i.e., it satisfies Slater's constraint qualification.*

*Proof of Proposition 3:* Consider a point  $\mathbf{p}^0$  that satisfies Assumption 1 (in particular,  $\boldsymbol{\pi}^0 = \mathbf{1}$  holds). Constraints (6b), (6c), (6d), and (7) can be written in the form of a block diagonal matrix inequality (8b). The implication is that  $\mathcal{G}(\mathbf{p}^0)$  is negative definite, i.e., all its eigenvalues are negative. By continuity of the eigenvalues as functions of the matrix elements [35, Appendix D], there is a ball of sufficiently small

radius around  $\mathbf{p}^0$  such that for all  $\mathbf{p}$  in this ball, the eigenvalues of  $\mathcal{G}(\mathbf{p})$  remain negative. Any point within the ball satisfying  $\boldsymbol{\pi} < \mathbf{1}$  together with the associated  $\mathbf{S}, \boldsymbol{\zeta}, \mathbf{Z}$  yields a strictly feasible point for constraints (6b), (6c), (6d), and (7). ■

### A. SCA using difference of convex functions (SCA-1)

The main idea is to replace (6b) with a surrogate convex inequality constraint. To this end, the left-hand side of (6b) is replaced by a convex function in the variables  $\mathbf{Z}, \boldsymbol{\Pi}$ , which is denoted by  $\mathcal{C}(\boldsymbol{\Pi}, \mathbf{Z}; \boldsymbol{\Pi}_0, \mathbf{Z}_0)$ , where  $\boldsymbol{\Pi}_0, \mathbf{Z}_0$  are given matrices to be specified later. This approach has been investigated in the context of BMIs for control problems with bilinearities arising in output feedback control problems; see [36]. We first define the following linear function of  $\boldsymbol{\Pi}, \mathbf{Z}$  with parameters  $\boldsymbol{\Pi}_0, \mathbf{Z}_0$

$$\begin{aligned}
\mathcal{H}_{\text{lin}}(\boldsymbol{\Pi}, \mathbf{Z}; \boldsymbol{\Pi}_0, \mathbf{Z}_0) &= \\
&+ \mathbf{B}_u \boldsymbol{\Pi}_0 \boldsymbol{\Pi}_0^\top \mathbf{B}_u^\top - \mathbf{B}_u \boldsymbol{\Pi} \boldsymbol{\Pi}_0^\top \mathbf{B}_u^\top - \mathbf{B}_u \boldsymbol{\Pi}_0 \boldsymbol{\Pi}^\top \mathbf{B}_u^\top \\
&+ \mathbf{B}_u \boldsymbol{\Pi}_0 \mathbf{Z}_0^\top - \mathbf{B}_u \boldsymbol{\Pi} \mathbf{Z}_0^\top - \mathbf{B}_u \boldsymbol{\Pi}_0 \mathbf{Z}^\top \\
&+ \mathbf{Z}_0^\top \boldsymbol{\Pi}_0 \mathbf{B}_u^\top - \mathbf{Z}_0^\top \boldsymbol{\Pi} \mathbf{B}_u^\top - \mathbf{Z}^\top \boldsymbol{\Pi}_0 \mathbf{B}_u^\top \\
&+ \mathbf{Z}_0^\top \mathbf{Z}_0 - \mathbf{Z}_0^\top \mathbf{Z} - \mathbf{Z}^\top \mathbf{Z}_0. \quad (22)
\end{aligned}$$

The function  $\mathcal{C}(\boldsymbol{\Pi}, \mathbf{Z}; \boldsymbol{\Pi}_0, \mathbf{Z}_0)$  is given by

$$\mathcal{C}(\cdot) = \begin{bmatrix} \mathbf{A} \mathbf{S} + \mathbf{S} \mathbf{A}^\top + 2\alpha \mathbf{S} \\ + \frac{1}{2} (\mathbf{B}_u \boldsymbol{\Pi} - \mathbf{Z}^\top) (\mathbf{B}_u \boldsymbol{\Pi} - \mathbf{Z}^\top)^\top \\ + \frac{1}{2} \mathcal{H}_{\text{lin}}(\boldsymbol{\Pi}, \mathbf{Z}; \boldsymbol{\Pi}_0, \mathbf{Z}_0) & \mathbf{B}_w \\ \mathbf{B}_w^\top & -2\alpha \mathbf{I} \end{bmatrix}. \quad (23)$$

The following proposition asserts that  $\mathcal{C}(\boldsymbol{\Pi}, \mathbf{Z}; \boldsymbol{\Pi}_0, \mathbf{Z}_0)$  is a convex function that upper bounds the left-hand side of (6b).

**Proposition 4.** *It holds for all  $\boldsymbol{\Pi}, \mathbf{Z}$  and  $\boldsymbol{\Pi}_0, \mathbf{Z}_0$  that*

$$\begin{bmatrix} \mathbf{A} \mathbf{S} + \mathbf{S} \mathbf{A}^\top + 2\alpha \mathbf{S} & \\ -\mathbf{B}_u \boldsymbol{\Pi} \mathbf{Z} - \mathbf{Z}^\top \boldsymbol{\Pi} \mathbf{B}_u^\top & \mathbf{B}_w \\ \mathbf{B}_w^\top & -2\alpha \mathbf{I} \end{bmatrix} \preceq \mathcal{C}(\boldsymbol{\Pi}, \mathbf{Z}; \boldsymbol{\Pi}_0, \mathbf{Z}_0), \quad (24)$$

and  $\mathcal{C}(\boldsymbol{\Pi}, \mathbf{Z}; \boldsymbol{\Pi}_0, \mathbf{Z}_0)$  is convex in  $\boldsymbol{\Pi}, \mathbf{Z}$ .

*Proof of Proposition 4:* To construct the upper bound (24), the bilinear term is written as

$$\begin{aligned}
-\mathbf{B}_u \boldsymbol{\Pi} \mathbf{Z} - \mathbf{Z}^\top \boldsymbol{\Pi} \mathbf{B}_u^\top &= \frac{1}{2} \left[ (\mathbf{B}_u \boldsymbol{\Pi} - \mathbf{Z}^\top) (\mathbf{B}_u \boldsymbol{\Pi} - \mathbf{Z}^\top)^\top \right. \\
&\quad \left. - (\mathbf{B}_u \boldsymbol{\Pi} + \mathbf{Z}^\top) (\mathbf{B}_u \boldsymbol{\Pi} + \mathbf{Z}^\top)^\top \right] \quad (25)
\end{aligned}$$

The term  $(\mathbf{B}_u \boldsymbol{\Pi} - \mathbf{Z}^\top) (\mathbf{B}_u \boldsymbol{\Pi} - \mathbf{Z}^\top)^\top$  is convex in  $\mathbf{Z}$  and  $\boldsymbol{\Pi}$  since it comes from an affine transformation of the domain of a convex function [37, Example 3.48]. The term

$$\mathcal{H}(\boldsymbol{\Pi}, \mathbf{Z}) := -(\mathbf{B}_u \boldsymbol{\Pi} + \mathbf{Z}^\top) (\mathbf{B}_u \boldsymbol{\Pi} + \mathbf{Z}^\top)^\top$$

is concave in  $\mathbf{Z}$  and  $\boldsymbol{\Pi}$ . We can therefore invoke the fact that the first-order Taylor approximation of a concave function (at any point) is a global over-estimator of the function. Let  $\boldsymbol{\Pi}_0, \mathbf{Z}_0$  be the linearization point, and let  $\mathcal{H}_{\text{lin}}(\boldsymbol{\Pi}, \mathbf{Z}; \boldsymbol{\Pi}_0, \mathbf{Z}_0)$  denote the linearization of  $\mathcal{H}(\boldsymbol{\Pi}, \mathbf{Z})$  at the point  $(\boldsymbol{\Pi}_0, \mathbf{Z}_0)$ . It holds that

$$\mathcal{H}(\boldsymbol{\Pi}, \mathbf{Z}) \preceq \mathcal{H}_{\text{lin}}(\boldsymbol{\Pi}, \mathbf{Z}; \boldsymbol{\Pi}_0, \mathbf{Z}_0) \quad (26)$$

for all  $\mathbf{\Pi}_0, \mathbf{Z}_0$  and  $\mathbf{\Pi}, \mathbf{Z}$ .

The linearization can be derived by substituting  $\mathbf{\Pi} = \mathbf{\Pi}_0 + (\mathbf{\Pi} - \mathbf{\Pi}_0)$  and  $\mathbf{Z} = \mathbf{Z}_0 + (\mathbf{Z} - \mathbf{Z}_0)$  into  $\mathcal{H}(\mathbf{\Pi}, \mathbf{Z})$  and ignoring all second-order terms that involve  $(\mathbf{\Pi} - \mathbf{\Pi}_0)$  and  $(\mathbf{Z} - \mathbf{Z}_0)$ . The result is (22). Combining (22) with (26) and (25), we conclude that the left-hand side of (6b) is upperbounded as

$$\begin{aligned} & \begin{bmatrix} \mathbf{AS} + \mathbf{SA}^\top + 2\alpha\mathbf{S} & & \\ -\mathbf{B}_u\mathbf{\Pi}\mathbf{Z} - \mathbf{Z}^\top\mathbf{\Pi}\mathbf{B}_u^\top & \mathbf{B}_w & \\ & \mathbf{B}_w^\top & -2\alpha\mathbf{I} \end{bmatrix} \\ & \succeq \begin{bmatrix} \mathbf{AS} + \mathbf{SA}^\top + 2\alpha\mathbf{S} & & \\ +\frac{1}{2}(\mathbf{B}_u\mathbf{\Pi} - \mathbf{Z}^\top)(\mathbf{B}_u\mathbf{\Pi} - \mathbf{Z}^\top)^\top & & \\ +\frac{1}{2}\mathcal{H}_{\text{lin}}(\mathbf{\Pi}, \mathbf{Z}; \mathbf{\Pi}_0, \mathbf{Z}_0) & & \\ & \mathbf{B}_w & \\ & \mathbf{B}_w^\top & -2\alpha\mathbf{I} \end{bmatrix}. \quad (27) \end{aligned}$$

This can be obtained using the fact that

$$\begin{bmatrix} \mathbf{A}_1 & \mathbf{B} \\ \mathbf{B}^\top & \mathbf{C} \end{bmatrix} \succeq \mathbf{O}, \mathbf{A}_2 \succeq \mathbf{A}_1 \implies \begin{bmatrix} \mathbf{A}_2 & \mathbf{B} \\ \mathbf{B}^\top & \mathbf{C} \end{bmatrix} \succeq \mathbf{O}$$

which can be proved using the definition of positive semidefiniteness. Inequality (27) holds for all  $\mathbf{\Pi}_0, \mathbf{Z}_0$  and  $\mathbf{\Pi}, \mathbf{Z}$ , and its left-hand side is  $\mathcal{C}(\mathbf{\Pi}, \mathbf{Z}; \mathbf{\Pi}_0, \mathbf{Z}_0)$ . ■

Therefore, a convex approximation of the BMI is obtained by replacing constraint (6b) with the convex constraint  $\mathcal{C}(\mathbf{\Pi}, \mathbf{Z}; \mathbf{\Pi}_0, \mathbf{Z}_0) \preceq \mathbf{O}$ . The resulting problem has a restricted feasible set due to (24). Although  $\mathcal{C}(\mathbf{\Pi}, \mathbf{Z}; \mathbf{\Pi}_0, \mathbf{Z}_0)$  is a convex function in  $\mathbf{\Pi}$  and  $\mathbf{Z}$ , it is not linear in  $\mathbf{\Pi}$  and  $\mathbf{Z}$ . Therefore, when we replace (6b) by the constraint  $\mathcal{C}(\mathbf{\Pi}, \mathbf{Z}; \mathbf{\Pi}_0, \mathbf{Z}_0) \preceq \mathbf{O}$ , a convex constraint is obtained, but not an LMI. Fortunately, the constraint  $\mathcal{C}(\mathbf{\Pi}, \mathbf{Z}; \mathbf{\Pi}_0, \mathbf{Z}_0) \preceq \mathbf{O}$  can be equivalently written as an LMI as follows.

**Lemma 2.** *It holds that*

$$\begin{aligned} \mathcal{C}(\mathbf{\Pi}, \mathbf{Z}; \mathbf{\Pi}_0, \mathbf{Z}_0) \preceq \mathbf{O} & \iff \mathcal{C}_s(\mathbf{\Pi}, \mathbf{Z}; \mathbf{\Pi}_0, \mathbf{Z}_0) = \\ & \begin{bmatrix} \mathbf{AS} + \mathbf{SA}^\top + 2\alpha\mathbf{S} & & & \\ +\frac{1}{2}\mathcal{H}_{\text{lin}}(\mathbf{\Pi}, \mathbf{Z}; \mathbf{\Pi}_0, \mathbf{Z}_0) & \frac{1}{\sqrt{2}}(\mathbf{B}_u\mathbf{\Pi} - \mathbf{Z}^\top) & \mathbf{B}_w & \\ \frac{1}{\sqrt{2}}(\mathbf{B}_u\mathbf{\Pi} - \mathbf{Z}^\top)^\top & & -\mathbf{I} & \mathbf{O} \\ & \mathbf{B}_w^\top & \mathbf{O} & -2\alpha\mathbf{I} \end{bmatrix} \preceq \mathbf{O}. \quad (28) \end{aligned}$$

*Proof of Lemma 2:* Applying the Schur complement to  $\mathcal{C}(\mathbf{\Pi}, \mathbf{Z}; \mathbf{\Pi}_0, \mathbf{Z}_0) \preceq \mathbf{O}$  yields the LMI  $\mathcal{C}_s(\mathbf{\Pi}, \mathbf{Z}; \mathbf{\Pi}_0, \mathbf{Z}_0)$ . ■

To summarize, the convex approximation to (6) at  $\mathbf{\Pi}_0, \mathbf{Z}_0$  is formed by replacing the integer constraints by the box constraints (7), and the BMI (6b) by the constraint the LMI in (28). This problem is stated as follows:

$$\hat{L} = \underset{\mathbf{S}, \mathbf{Z}, \zeta, \boldsymbol{\pi}}{\text{minimize}} \quad \zeta + \boldsymbol{\alpha}^\top \boldsymbol{\pi} \quad (29a)$$

$$\text{subject to} \quad (6c), (6d), (7), (28). \quad (29b)$$

Problem (29) is an SDP with optimal value denoted by  $\hat{L}$ , whose relationship with  $L$  is as follows.

**Corollary 2.** *The optimal value of the convex approximation (29) for all  $\mathbf{\Pi}_0, \mathbf{Z}_0$  is an upper bound on the optimal value of (8), that is,  $L \leq \hat{L}$ .*

*Proof of Corollary 2:* Due to (24) and (28), problem (29) has a restricted feasible set with respect to problem (8). ■

The convex approximation (29) depends on the point  $\mathbf{\Pi}_0, \mathbf{Z}_0$ , and can be successively improved. The main idea is to solve a sequence of convex approximations given by (29), where the values of  $\mathbf{\Pi}_0, \mathbf{Z}_0$  for the next approximating problem are given by the solution of the previous problem.

Let  $k = 1, 2, \dots$  denote the index of the convex approximation to be solved, and let  $\mathbf{S}_k, \zeta_k, \mathbf{\Pi}_k, \mathbf{Z}_k$  denote its solution. The  $k$ -th problem is obtained by adding a strictly convex regularizer to the objective (29a), which ensures that the problem has a unique solution. The  $k$ -th problem is thus

$$\hat{L}_k^{(1)} = \underset{\{\mathbf{S}, \mathbf{Z}, \zeta, \boldsymbol{\pi}\}}{\text{minimize}} \quad \zeta + \boldsymbol{\alpha}^\top \boldsymbol{\pi} + \rho J_k \quad (30a)$$

$$\text{subject to} \quad \mathcal{C}_s(\mathbf{\Pi}, \mathbf{Z}; \mathbf{\Pi}_{k-1}, \mathbf{Z}_{k-1}) \preceq \mathbf{O} \quad (30b)$$

$$(6c), \mathbf{H}\boldsymbol{\pi} \leq \mathbf{h}, \quad 0 \leq \boldsymbol{\pi} \leq 1, \quad (30c)$$

where  $J_k = \|\zeta - \zeta_{k-1}\|_2^2 + \|\mathbf{S} - \mathbf{S}_{k-1}\|_F^2 + \|\mathbf{Z} - \mathbf{Z}_{k-1}\|_F^2 + \|\mathbf{\Pi} - \mathbf{\Pi}_{k-1}\|_F^2$ ; the linearization point is given by  $\mathbf{\Pi}_0 = \mathbf{\Pi}_{k-1}, \mathbf{Z}_0 = \mathbf{Z}_{k-1}$ ;  $\rho$  is the weight of the quadratic regularizers. For  $k = 1$ , the point  $\mathbf{\Pi}_0, \mathbf{Z}_0$  can be selected as any interior point of (8); such is guaranteed to exist due to Proposition 3.

Notice that for every  $k$ , problem (30) has the form of (8), but the objective is a strictly convex quadratic, and the constraint function is convex. The convergence is established in the following proposition.

**Proposition 5.** *Let  $\mathbf{p}_k, \boldsymbol{\Lambda}_k$  denote a KKT point of (30). Suppose that the feasible set of (8) is bounded, and that the following hold for problem (30) for  $k = 1, 2, 3, \dots$*

- i) Slater's constraint qualification holds.
- ii) The Lagrange multiplier  $\boldsymbol{\Lambda}_k$  is locally unique.
- iii) Strict complementarity holds for the KKT point.
- iv) The second-order sufficiency condition holds for the KKT point.

Then, the following are concluded:

- a) It holds that  $f(\mathbf{p}_k) \geq L$  and  $L_k^{(1)} \geq L$  for  $k = 1, 2, 3, \dots$
- b) The sequence  $\{f(\mathbf{p}_k)\}_{k=1}^\infty$  is monotone decreasing, and converges to a limit  $\hat{f}^{(1)} \geq L$ .
- c) Every limit point of the sequence  $\{\mathbf{p}_k, \boldsymbol{\Lambda}_k\}_{k=1}^\infty$  is a KKT point of (8). If the set of KKT points of (8) is finite, then the entire sequence  $\{\mathbf{p}_k, \boldsymbol{\Lambda}_k\}_{k=1}^\infty$  converges to a KKT point of (8).

*Proof of Proposition 5:* Notice that problem (30) has the same feasible set as (29) (with  $\mathbf{\Pi}_0, \mathbf{Z}_0$  replaced by  $\mathbf{\Pi}_{k-1}, \mathbf{Z}_{k-1}$ ). Corollary 2 establishes that its feasible set is a restriction of the one in (8). It follows that  $f(\mathbf{p}_k) \geq L$ , and  $L_k^{(1)} \geq L$  holds because of the added regularizer in (30a). The monotonicity of  $\{f(\mathbf{p}_k)\}_{k=1}^\infty$  follows from a corresponding result in [36, Lemma 4.2(c)]. The sequence is thus monotone decreasing and bounded [the latter follows from the assumption on the boundedness of the feasible set of (8)]. It is a standard result in analysis that a bounded and monotone decreasing sequence has a limit. Therefore,  $\hat{f}^{(1)} \geq L$  holds for the limit due to  $f(\mathbf{p}_k) \geq L$ . The convergence result of part c) follows [36, Theorem 4.3]. It is emphasized that the existence of at least one limit point is guaranteed by the boundedness of the feasible set. ■

Albeit some of the conditions of the previous proposition may be hard to verify in practice, we encountered no case where the SCA algorithm did not converge. In particular, we tested the algorithm on a variety of dynamic systems with varying sizes and conditions in Section IX.

### B. Parametric SCA (SCA-2)

In this section, we depart from the difference of two convex functions approach used in the previous SCA, and use another approach to obtain an upper bound on the bilinear terms. The developments in this section follow the spirit of the methods presented in [38], where the authors investigate a new approach to solve BMIs that are often encountered in output feedback control problems.

First, let  $\mathcal{F}_1(\mathbf{p})$  denote the left-hand side of (6b). Given  $\mathbf{\Pi}_k$  and  $\mathbf{Z}_k$ , define  $\Delta\mathbf{\Pi} = \mathbf{\Pi} - \mathbf{\Pi}_k$  and  $\Delta\mathbf{Z} = \mathbf{Z} - \mathbf{Z}_k$ . For any  $\mathbf{Q} \in \mathbb{S}_{++}^{n_u}$ , define further the following function:

$$\begin{aligned} \mathcal{K}_1(\mathbf{p}; \mathbf{p}_k, \mathbf{Q}) = & \begin{bmatrix} -\mathbf{B}_u \mathbf{\Pi}_k \mathbf{Z}_k - \mathbf{Z}_k^\top \mathbf{\Pi}_k \mathbf{B}_u^\top & \mathbf{B}_w \\ \mathbf{B}_w^\top & -2\alpha \mathbf{I} \end{bmatrix} \\ & + \begin{bmatrix} \mathbf{A}\mathbf{S} + \mathbf{S}\mathbf{A}^\top + 2\alpha\mathbf{S} - \mathbf{B}_u \mathbf{\Pi}_k \Delta\mathbf{Z} & \mathbf{O} \\ -\Delta\mathbf{Z}^\top \mathbf{\Pi}_k \mathbf{B}_u^\top - \mathbf{B}_u \Delta\mathbf{\Pi} \mathbf{Z}_k - \mathbf{Z}_k^\top \Delta\mathbf{\Pi} \mathbf{B}_u^\top & \mathbf{O} \\ \mathbf{O} & \mathbf{O} \end{bmatrix} \\ & + \begin{bmatrix} \mathbf{B}_u \Delta\mathbf{\Pi} \mathbf{Q} \Delta\mathbf{\Pi} \mathbf{B}_u^\top + \Delta\mathbf{Z}^\top \mathbf{Q}^{-1} \Delta\mathbf{Z} & \mathbf{O} \\ \mathbf{O} & \mathbf{O} \end{bmatrix}. \end{aligned} \quad (31)$$

Similar to Proposition 4, an upper bound on  $\mathcal{F}_1(\mathbf{p})$  is provided by the next proposition.

**Proposition 6.** *It holds for all  $\mathbf{p}$ ,  $\mathbf{\Pi}_k$ ,  $\mathbf{Z}_k$  and  $\mathbf{Q} \in \mathbb{S}_{++}^{n_u}$  that*

$$\mathcal{F}_1(\mathbf{p}) \leq \mathcal{K}_1(\mathbf{p}; \mathbf{p}_k, \mathbf{Q}). \quad (32)$$

*Proof of Proposition 6:* Function  $\mathcal{F}_1(\mathbf{p})$  is written as

$$\begin{aligned} \mathcal{F}_1(\mathbf{p}) &= \mathcal{C}_0 + \mathcal{A}(\mathbf{p}) + \mathcal{B}(\mathbf{p}) \\ &= \begin{bmatrix} \mathbf{O} & \mathbf{B}_w \\ \mathbf{B}_w^\top & -2\alpha \mathbf{I} \end{bmatrix} + \begin{bmatrix} \mathbf{A}\mathbf{S} + \mathbf{S}\mathbf{A}^\top + 2\alpha\mathbf{S} & \mathbf{O} \\ \mathbf{O} & \mathbf{O} \end{bmatrix} \\ &+ \begin{bmatrix} -\mathbf{B}_u \mathbf{\Pi} \mathbf{Z} - \mathbf{Z}^\top \mathbf{\Pi} \mathbf{B}_u^\top & \mathbf{O} \\ \mathbf{O} & \mathbf{O} \end{bmatrix} \end{aligned}$$

Substituting  $\mathbf{\Pi} = \mathbf{\Pi}_k + \Delta\mathbf{\Pi} = \mathbf{\Pi}_k + \mathbf{\Pi} - \mathbf{\Pi}_k$  and  $\mathbf{Z} = \mathbf{Z}_k + \Delta\mathbf{Z} = \mathbf{Z}_k + \mathbf{Z} - \mathbf{Z}_k$  into  $\mathcal{B}(\mathbf{z})$  yields

$$\mathcal{B}(\mathbf{p}) = \begin{bmatrix} -\mathbf{B}_u (\mathbf{\Pi}_k + \Delta\mathbf{\Pi}) (\mathbf{Z}_k + \Delta\mathbf{Z}) & \mathbf{O} \\ -(\mathbf{Z}_k + \Delta\mathbf{Z})^\top (\mathbf{\Pi}_k + \Delta\mathbf{\Pi}) \mathbf{B}_u^\top & \mathbf{O} \\ \mathbf{O} & \mathbf{O} \end{bmatrix}$$

where  $-\mathbf{B}_u (\mathbf{\Pi}_k + \Delta\mathbf{\Pi}) (\mathbf{Z}_k + \Delta\mathbf{Z}) = -\mathbf{B}_u \mathbf{\Pi}_k \mathbf{Z}_k - \mathbf{B}_u \mathbf{\Pi}_k \Delta\mathbf{Z} - \mathbf{B}_u \Delta\mathbf{\Pi} \mathbf{Z}_k - \mathbf{B}_u \Delta\mathbf{\Pi} \Delta\mathbf{Z}$  and  $-(\mathbf{Z}_k + \Delta\mathbf{Z})^\top (\mathbf{\Pi}_k + \Delta\mathbf{\Pi}) \mathbf{B}_u^\top = -\mathbf{Z}_k^\top \mathbf{\Pi}_k \mathbf{B}_u^\top - \mathbf{Z}_k^\top \Delta\mathbf{\Pi} \mathbf{B}_u^\top - \Delta\mathbf{Z}^\top \mathbf{\Pi}_k \mathbf{B}_u^\top - \Delta\mathbf{Z}^\top \Delta\mathbf{\Pi} \mathbf{B}_u^\top$ .

Given this,  $\mathcal{B}(\mathbf{p})$  can be rearranged as

$$\begin{aligned} \mathcal{B}(\mathbf{p}) &= \begin{bmatrix} -\mathbf{B}_u \mathbf{\Pi}_k \mathbf{Z}_k - \mathbf{Z}_k^\top \mathbf{\Pi}_k \mathbf{B}_u^\top - \mathbf{B}_u \mathbf{\Pi}_k \Delta\mathbf{Z} & \mathbf{O} \\ -\Delta\mathbf{Z}^\top \mathbf{\Pi}_k \mathbf{B}_u^\top - \mathbf{B}_u \Delta\mathbf{\Pi} \mathbf{Z}_k - \mathbf{Z}_k^\top \Delta\mathbf{\Pi} \mathbf{B}_u^\top & \mathbf{O} \\ \mathbf{O} & \mathbf{O} \end{bmatrix} \\ &+ \begin{bmatrix} -\mathbf{B}_u \Delta\mathbf{\Pi} \Delta\mathbf{Z} - \Delta\mathbf{Z}^\top \Delta\mathbf{\Pi} \mathbf{B}_u^\top & \mathbf{O} \\ \mathbf{O} & \mathbf{O} \end{bmatrix} \end{aligned}$$

By combining and grouping these results, we obtain

$$\begin{aligned} \mathcal{F}_1(\mathbf{p}) &= \begin{bmatrix} -\mathbf{B}_u \mathbf{\Pi}_k \mathbf{Z}_k - \mathbf{Z}_k^\top \mathbf{\Pi}_k \mathbf{B}_u^\top & \mathbf{B}_w \\ \mathbf{B}_w^\top & -2\alpha \mathbf{I} \end{bmatrix} \\ &+ \begin{bmatrix} \mathbf{A}\mathbf{S} + \mathbf{S}\mathbf{A}^\top + 2\alpha\mathbf{S} - \mathbf{B}_u \mathbf{\Pi}_k \Delta\mathbf{Z} & \mathbf{O} \\ -\Delta\mathbf{Z}^\top \mathbf{\Pi}_k \mathbf{B}_u^\top - \mathbf{B}_u \Delta\mathbf{\Pi} \mathbf{Z}_k - \mathbf{Z}_k^\top \Delta\mathbf{\Pi} \mathbf{B}_u^\top & \mathbf{O} \\ \mathbf{O} & \mathbf{O} \end{bmatrix} \\ &+ \begin{bmatrix} -\mathbf{B}_u \Delta\mathbf{\Pi} \Delta\mathbf{Z} - \Delta\mathbf{Z}^\top \Delta\mathbf{\Pi} \mathbf{B}_u^\top & \mathbf{O} \\ \mathbf{O} & \mathbf{O} \end{bmatrix} \end{aligned}$$

An upper bound for the last bilinear term for any  $\mathbf{Q} \in \mathbb{S}_{++}^{n_u}$  is given as [38, Lemma 1]

$$\begin{aligned} & -\mathbf{B}_u \Delta\mathbf{\Pi} \Delta\mathbf{Z} - \Delta\mathbf{Z}^\top \Delta\mathbf{\Pi} \mathbf{B}_u^\top \preceq \\ & \mathbf{B}_u \Delta\mathbf{\Pi} \mathbf{Q} \Delta\mathbf{\Pi} \mathbf{B}_u^\top + \Delta\mathbf{Z}^\top \mathbf{Q}^{-1} \Delta\mathbf{Z}. \end{aligned}$$

Combining the previous two results yields (32).  $\blacksquare$

The previous proposition suggests that constraint (6b) can be replaced by  $\mathcal{K}_1(\mathbf{p}; \mathbf{p}_k, \mathbf{Q}) \preceq \mathbf{O}$ . There are two challenges to be addressed though. First, although  $\mathcal{K}_1(\mathbf{p}; \mathbf{p}_k, \mathbf{Q})$  is a convex function of  $\mathbf{p}$ , it is not linear, and thus constraint  $\mathcal{K}_1(\mathbf{p}; \mathbf{p}_k, \mathbf{Q}) \preceq \mathbf{O}$  is not an LMI. Second, although  $\mathbf{Q}$  can remain constant, the approximation can be tightened if  $\mathbf{Q}$  is allowed to be an optimization variable. The former challenge is addressed by Lemma 3, which is analogous to Lemma 2.

**Lemma 3.** *Constraint  $\mathcal{K}_1(\mathbf{p}; \mathbf{p}_k, \mathbf{Q}) \preceq \mathbf{O}$  is equivalent to*

$$\mathcal{K}(\mathbf{p}; \mathbf{p}_k, \mathbf{Q}) = \begin{bmatrix} \mathcal{O}(\mathbf{p}; \mathbf{p}_k) & \mathbf{B}_w & \mathbf{B}_u \Delta\mathbf{\Pi} & \Delta\mathbf{Z}^\top \\ \mathbf{B}_w^\top & -2\alpha \mathbf{I} & \mathbf{O} & \mathbf{O} \\ \Delta\mathbf{\Pi} \mathbf{B}_u^\top & \mathbf{O} & -\mathbf{Q}^{-1} & \mathbf{O} \\ \Delta\mathbf{Z} & \mathbf{O} & \mathbf{O} & -\mathbf{Q} \end{bmatrix} \preceq \mathbf{O}, \quad (33)$$

$$\begin{aligned} \mathcal{O}(\mathbf{p}; \mathbf{p}_k) &= -\mathbf{B}_u \mathbf{\Pi}_k \mathbf{Z}_k - \mathbf{Z}_k^\top \mathbf{\Pi}_k \mathbf{B}_u^\top + \mathbf{A}\mathbf{S} + \mathbf{S}\mathbf{A}^\top + 2\alpha\mathbf{S} \\ &- \mathbf{B}_u \mathbf{\Pi}_k \Delta\mathbf{Z} - \Delta\mathbf{Z}^\top \mathbf{\Pi}_k \mathbf{B}_u^\top - \mathbf{B}_u \Delta\mathbf{\Pi} \mathbf{Z}_k - \mathbf{Z}_k^\top \Delta\mathbf{\Pi} \mathbf{B}_u^\top. \end{aligned}$$

*Proof of Lemma 3:* Use the Schur complement.  $\blacksquare$

When  $\mathbf{Q}$  is an optimization variable, function  $\mathcal{K}(\mathbf{p}; \mathbf{p}_k, \mathbf{Q})$  is not convex in  $\mathbf{p}$  and  $\mathbf{Q}$ . An upper bound of  $\mathcal{K}(\mathbf{p}; \mathbf{p}_k, \mathbf{Q})$  that is linear in  $\mathbf{p}$  and  $\mathbf{Q}$  is given in Lemma 5. The following lemma gives a particular matrix property that becomes the foundation for Lemma 5.

**Lemma 4.** *Let  $\mathcal{Q}(\mathbf{x}) : \mathbb{R}^n \rightarrow \mathbb{S}_{++}^m$  be a mapping defined as  $\mathcal{Q}(\mathbf{x}) = \sum_{i=1}^n x_i \mathcal{Q}_i$  where  $\mathcal{Q}_i \in \mathbb{S}^m$ . The following inequality holds, where the right-hand side is the linearization of  $-\mathcal{Q}(\mathbf{x})^{-1}$  around  $\mathbf{x}_k$ :*

$$-\mathcal{Q}(\mathbf{x})^{-1} \preceq -2\mathcal{Q}(\mathbf{x}_k)^{-1} + \mathcal{Q}(\mathbf{x}_k)^{-1} \mathcal{Q}(\mathbf{x}) \mathcal{Q}(\mathbf{x}_k)^{-1}. \quad (34)$$

*Proof of Lemma 4:* Let  $\mathcal{R}(\mathbf{x}; \mathbf{x}_k)$  be the first-order Taylor approximation of  $-\mathcal{Q}(\mathbf{x})^{-1}$  computed around  $\mathbf{x}_k$ . That is

$$\mathcal{R}(\mathbf{x}; \mathbf{x}_k) = -\mathcal{Q}(\mathbf{x}_k)^{-1} - [D\mathcal{Q}(\mathbf{x}_k)^{-1}](\mathbf{x} - \mathbf{x}_k). \quad (35)$$

By setting  $\Delta\mathbf{x} = \mathbf{x} - \mathbf{x}_k$ , the differential  $-[D\mathcal{Q}(\mathbf{x}_k)^{-1}]\Delta\mathbf{x}$  is given by [39]

$$\begin{aligned} [D\mathcal{Q}(\mathbf{x}_k)^{-1}]\Delta\mathbf{x} &= -\mathcal{Q}(\mathbf{x}_k)^{-1} [D\mathcal{Q}(\mathbf{x}_k)] \Delta\mathbf{x} \mathcal{Q}(\mathbf{x}_k)^{-1} \\ &= -\mathcal{Q}(\mathbf{x}_k)^{-1} \sum_{i=1}^n \frac{\partial \mathcal{Q}(\mathbf{x}_k)}{\partial x_i} \Delta x_i \mathcal{Q}(\mathbf{x}_k)^{-1} \\ &= -\mathcal{Q}(\mathbf{x}_k)^{-1} \mathcal{Q}(\mathbf{x}) \mathcal{Q}(\mathbf{x}_k)^{-1} + \mathcal{Q}(\mathbf{x}_k)^{-1}. \end{aligned}$$

Substituting the latter into (35) yields

$$\mathcal{R}(\mathbf{x}; \mathbf{x}_k) = -2\mathcal{Q}(\mathbf{x}_k)^{-1} + \mathcal{Q}(\mathbf{x}_k)^{-1}\mathcal{Q}(\mathbf{x})\mathcal{Q}(\mathbf{x}_k)^{-1}.$$

Since  $\mathcal{Q}(\mathbf{x})$  is positive definite, then it follows that  $-\mathcal{Q}(\mathbf{x})^{-1}$  is concave [37, Example 3.48]. Because the first-order approximation of a concave function is a global over-estimator, we obtain (34). ■

**Lemma 5.** *It holds for all  $\mathbf{p}$ ,  $\mathbf{Q} \in \mathbb{S}_{++}^{n_u}$ ,  $\mathbf{\Pi}_k, \mathbf{Z}_k$ , and  $\mathbf{Q}_k \in \mathbb{S}_{++}^{n_u}$  that*

$$\mathcal{K}(\mathbf{p}; \mathbf{p}_k, \mathbf{Q}) \preceq \mathcal{K}_s(\mathbf{p}, \mathbf{Q}; \mathbf{p}_k, \mathbf{Q}_k) \quad (36)$$

where  $\mathcal{K}_s(\mathbf{p}, \mathbf{Q}; \mathbf{p}_k, \mathbf{Q}_k) =$

$$\begin{bmatrix} \Omega(\mathbf{p}; \mathbf{p}_k) & \mathbf{B}_w & \mathbf{B}_u \Delta \mathbf{\Pi} \mathbf{Q}_k & \Delta \mathbf{Z}^\top \\ \mathbf{B}_w^\top & -2\alpha \mathbf{I} & \mathbf{O} & \mathbf{O} \\ \mathbf{Q}_k \Delta \mathbf{\Pi} \mathbf{B}_u^\top & \mathbf{O} & -2\mathbf{Q}_k + \mathbf{Q} & \mathbf{O} \\ \Delta \mathbf{Z} & \mathbf{O} & \mathbf{O} & -\mathbf{Q} \end{bmatrix}. \quad (37)$$

*Proof of Lemma 5:* By linearizing  $-\mathbf{Q}^{-1}$  around a given  $\mathbf{Q}_k \in \mathbb{S}_{++}^{n_u}$ , an upper bound on  $\mathcal{K}(\mathbf{p}; \mathbf{p}_k, \mathbf{Q})$  can be derived as follows. Since  $-\mathbf{Q}^{-1}$  is concave in  $\mathbf{Q}$ , then according to Lemma 4, the over approximation of  $-\mathbf{Q}^{-1}$  around  $\mathbf{Q}_k$  is  $-\mathbf{Q}_k^{-1} + \mathbf{Q}_k^{-1}\mathbf{Q}\mathbf{Q}_k^{-1}$ . Substituting this over approximation of  $-\mathbf{Q}^{-1}$  into  $\mathcal{K}(\mathbf{p}; \mathbf{p}_k, \mathbf{Q})$  and applying congruence transformation with  $\text{diag}(\mathbf{I}, \mathbf{I}, \mathbf{Q}_k, \mathbf{I})$  as the post and pre-multiplier yields (37). The relation in (36) is obtained due to the fact that  $-\mathbf{Q}^{-1} \preceq -\mathbf{Q}_k^{-1} + \mathbf{Q}_k^{-1}\mathbf{Q}\mathbf{Q}_k^{-1}$ . ■

Thus the constraint  $\mathcal{K}_s(\mathbf{p}, \mathbf{Q}; \mathbf{p}_k, \mathbf{Q}_k) \preceq \mathbf{O}$  yields a restricted feasible set relative to constraint (5b). Similarly to Section VI-A,  $k = 1, 2, 3, \dots$  is the index of the optimization problem to be solved, and  $\mathbf{p}_k, \mathbf{Q}_k$  denotes its solution. The  $k$ -th problem is an SDP and is stated as follows.

$$\hat{L}_k^{(2)} = \underset{\{\mathbf{S}, \mathbf{Z}, \zeta, \boldsymbol{\pi}, \mathbf{Q}\}}{\text{minimize}} \quad \zeta + \boldsymbol{\alpha}^\top \boldsymbol{\pi} + \rho J_k \quad (38a)$$

$$\text{subject to} \quad \mathcal{K}_s(\mathbf{p}, \mathbf{Q}; \mathbf{p}_{k-1}, \mathbf{Q}_{k-1}) \preceq \mathbf{O} \quad (38b)$$

$$c_1 \mathbf{I} \preceq \mathbf{Q} \preceq c_2 \mathbf{I}, \quad -2\mathbf{Q}_{k-1} + \mathbf{Q} \preceq -c_3 \mathbf{I} \quad (38c)$$

$$(\mathbf{6c}), \quad \mathbf{H}\boldsymbol{\pi} \preceq \mathbf{h}, \quad \mathbf{0} \leq \boldsymbol{\pi} \leq \mathbf{1}, \quad (38d)$$

where  $\rho, c_1, c_2$ , and  $c_3$  are positive constants, and  $J_k$  is the same regularizer as the one in (30). Constraint (38c) guarantees that  $\mathbf{Q}$  is positive definite, sequence  $\{\mathbf{Q}_k\}_{k=1}^\infty$  is bounded, and that  $-2\mathbf{Q}_k + \mathbf{Q}$ , which appears as a diagonal block in (37) is negative definite for all  $k$ . Similar to the first convex approximation, the above problem can be initialized by letting  $\{\mathbf{S}_0, \mathbf{Z}_0, \zeta_0, \boldsymbol{\pi}_0\}$  be any interior point of (8) and  $\mathbf{Q}_0 = \mathbf{I}$ . The algorithm convergence is characterized by the following proposition.

**Proposition 7.** *Assume that the MFCQ holds for every feasible point of (8) and that the sequence  $\{\mathbf{p}_k\}_{k=1}^\infty$  is bounded. Then, the following are concluded:*

- It holds that  $f(\mathbf{p}_k) \geq L$  and  $L_k^{(2)} \geq L$  for  $k = 1, 2, \dots$
- The sequence  $\{f(\mathbf{p}_k)\}_{k=1}^\infty$  is monotone decreasing, and converges to a limit  $f^{(2)} \geq L$ .
- Every limit point of  $\{\mathbf{p}_k\}_{k=1}^\infty$  is a stationary point of (8).

*Proof of Proposition 7:* The feasible set of problem (38) is a restriction of the one in (8) due to Proposition 6, Lemma 3, Lemma 5. It therefore holds that  $f(\mathbf{p}_k) \geq L$ , and  $L_k^{(2)} \geq L$

follows from the addition of the regularizer in the objective. The monotonicity of  $\{f(\mathbf{p}_k)\}_{k=1}^\infty$  follows from a related result in [38, Lemma 6]. The monotonicity and the boundedness imply the existence of the limit, similarly to Proposition 5. The convergence in part c) is analogous to [38, Proposition 5]. The existence of at least one limit point is ensured by the boundedness of the sequence  $\{\mathbf{p}_k\}_{k=1}^\infty$ . ■

Algorithm 2 in Appendix C provides the option to implement one of the two developed convex approximations [cf. (30) and (38)] in an iterative fashion with specific stopping criteria. The next section compares the two approximations in terms of computational effort and their convergence claims.

### C. Comparing the SCAs and Important Remarks

The first convex approximation is simpler to implement and involves a smaller number of SDP constraints and variables; see the difference in dimensions between constraints  $\mathcal{K}_s(\mathbf{p}, \mathbf{Q}; \mathbf{z}_k, \mathbf{Q}_k) \preceq \mathbf{O}$  and  $\mathcal{C}_s(\mathbf{\Pi}, \mathbf{Z}; \mathbf{\Pi}_k, \mathbf{Z}_k) \preceq \mathbf{O}$ . In addition, constraint (38c) is added, and an extra variable  $\mathbf{Q}$  is needed in (38). Hence, it is expected that the first convex approximation (30) requires less computational time.

Both methods rely on constructing a series of feasible sets that are subsets of the original nonconvex feasible set in (8). Each produces a sequence of decreasing objective values  $\{f(\mathbf{p}_k)\}_{k=1}^\infty$ , yielding upper bounds on the optimal value of (8).

It is also worth noting that the first method requires a constraint qualification and additional assumptions on the KKT point to hold for each convex approximation problem  $k$ . Slater's constraint qualification is also an assumption in one of the earliest SCA methods for nonlinear programming [40]. On the other hand, the second method requires only the MFCQ to hold for the original nonconvex problem (8). Both methods have a boundedness assumption; the first method requires the feasible set of (8) to be bounded, the second method only the resulting sequence to be bounded. The boundedness assumption respectively guarantees the existence of at least one limit point of  $\{\mathbf{p}_k\}_{k=1}^\infty$ . Both methods enjoy the property that every limit point of  $\{\mathbf{p}_k\}_{k=1}^\infty$  is a stationary point of (8).

**Remark 4** (Existence of Local Minima). *The stationarity is a necessary condition for local optimality (cf. Lemma 1). It is thus not guaranteed that the stationary point is indeed locally optimal. In view of the fact that the methods attempt to solve a nonconvex problem, such a convergence result is to be expected. It is worth asking whether the resulting limit point is indeed locally optimal. Sufficient conditions for local optimality of stationary points of nonlinear SDPs have been derived in the literature; see for example [32, Theorem 9].*

**Remark 5** (Recovering the Optimal Solution of (8)). *A comparison with the SDP relaxation of Section V is in order. The method of Section V produces a lower bound  $\hat{L}$  for the optimal value  $L$  of (8). The methods of this section derive upper bounds ( $\hat{L}^{(1)}$  or  $\hat{L}^{(2)}$ ) of  $L$ . Therefore, if the difference between the upper and lower bounds is small, we can assert that we have approximately solved nonconvex problem (8).*

#### D. Recovering the Integer Solutions

Appendix D presents a simple algorithm and a discussion on recovering the integer solutions of the actuator selection from the continuous ones that is generated via (17), (30), and (38). The relationship between the recovered integer solutions and the continuous ones is also discussed in Appendix D.

#### VII. SAA SELECTION VIA MISDP AND BIG-M METHOD

This section develops an alternative method for solving the optimization problem (5). This alternative can also be applied to other time-varying SaA selection problems with the control and estimation metrics and formulations in Tables VII and VIII in Appendix E.

As discussed in the previous sections, the mixed-integer bilinear term  $B_u \Pi Z + Z^T \Pi B_u^T$  is the term that renders the problem nonconvex. An alternative to solving the convex relaxations/approximations is to simply apply the Big-M method on the bilinear term. This technique has been used before for mixed-integer SDPs in the context of multi-vehicle path planning [41], and more recently for linear systems with Gaussian disturbances and for Kalman filtering [20].

In order to state the Big-M method, we will use the block matrices defined in (12)–(14). In particular, notice that due to the binary nature of  $\pi_i$ , constraint (14) can be equivalently written for all  $l, m$  as

$$G_{i,(l,m)} = \begin{cases} \pi_i Z_{i,(l,m)}, & \text{if } \pi_i = 1 \\ 0, & \text{if } \pi_i = 0. \end{cases} \quad (39)$$

By introducing a sufficiently large constant  $M$ , it is shown that the previous constraint can be equivalently written as

$$|G_{i,(l,m)} - Z_{i,(l,m)}| \leq M(1 - \pi_i), |G_{i,(l,m)}| \leq M\pi_i \quad (40)$$

**Lemma 6.** *Under the constraint  $\pi_i \in \{0, 1\}$  for all  $i$  and for sufficiently large  $M$ , then any  $Z$  and  $G$  satisfying (39) also satisfy (40), and vice versa.*

*Proof of Lemma 6:* Suppose that  $\pi_i = 1$ . Then, both (39) and (40) are equivalent to  $G_{i,(l,m)} = Z_{i,(l,m)}$  for all  $(l, m)$ . Suppose now that  $\pi_i = 0$ . Then, both (39) and (40) are equivalent to  $G_{i,(l,m)} = 0$  for all  $(l, m)$  and allow  $Z_{i,(l,m)}$  to be free. Notice that the proof indicates how big the constant  $M$  should be. In particular, it must be larger than the maximum entry of matrix  $Z$  that is the optimal solution of (5). In practice, a very large number is selected. ■

The advantage of (40) is that it converts the bilinear constraint (14) to a constraint linear in  $Z$ ,  $G$  and  $\Pi$ . Therefore, the actuator selection problem for  $\mathcal{L}_\infty$  control is written as

$$B_M^* = \underset{\{S, Z, \zeta, \pi, G\}}{\text{minimize}} \quad \zeta + \alpha_\pi^T \pi \quad (41a)$$

$$\text{subject to} \quad \begin{bmatrix} AS + SA^T + 2\alpha S & & & \\ -B_u G - G^T B_u^T & B_w & & \\ & B_w^T & & -2\alpha I \end{bmatrix} \preceq O \quad (41b)$$

$$\begin{bmatrix} -S & O & SC_z^T \\ O & -I & D_{wz}^T \\ C_z S & D_{wz} & -\zeta I \end{bmatrix} \preceq O \quad (41c)$$

$$H\pi \leq h, \quad \pi \in \{0, 1\}^N \quad (41d)$$

$$\Theta_1 G + \Theta_2 Z \leq L_M(\pi). \quad (41e)$$

The last constraint in (41) represents the vectorization of the Big-M constraints in (40), where  $\Theta_1$ ,  $\Theta_2$  and  $L(\pi)$  are suitable matrices, and the latter is a linear mapping in  $\pi$  that depends on  $M$ . The optimization still includes the integrality constraints on  $\pi$ , and hence it is a mixed-integer semidefinite program (MISDP). The key point is that it is equivalent to (5).

**Proposition 8.** *For sufficiently big  $M$ , problems (41) and (5) are equivalent, and thus, have equal optimal values, i.e.,  $f^* = B_M^*$ .*

*Proof of Proposition 8:* Introduce the change of variables  $G = \Pi Z$  in (5). The resulting problem and (41) have the same feasible sets due to Lemma 6. ■

The widely used convex optimization modeling toolboxes CVX and YALMIP have been expanded to incorporate modeling of mixed-integer convex programs [42], [43] and interface corresponding general-purpose SDP solvers combined with implementations of branch-and-bound (BB) methods. The BB method is essentially a smart and efficient way to run an exhaustive search over all possible  $2^N$  combinations of the binary variables. At most  $2^N$  SDPs are then solved in the worst case run of a BB method. However, the empirical complexity of BB algorithms is much smaller than the worst-case one, and thus, they are among the state-of-the-art in solving mixed-integer convex programs. Thus in principle, such off-the-shelf solvers can be applied to (41).

Unfortunately, it is unclear whether a BB algorithm would outperform the convex approximations derived in Section VI in terms of the quality of the solution, computational speed, and impact on the closed-loop system. For this purpose, we compare the performance of YALMIP's BB algorithm with the developed relaxations and approximations (SDP-R, SCA-1, SCA-2) in Section IX. Indeed, the authors in [41] points out that general-purpose MISDP solvers often suffer from low-quality solutions, and our tests indicate that the closed-loop performance of the controller resulting from the Big-M approach is unsatisfactory, when compared with SDP-R and SCAs. Specifically, the quality of the solution depends on the value of  $M$  that bounds  $G$  and  $Z$ . Hence, selecting a large  $M$  might cause numerical issues in terms of the computations of the optimization variable  $S$ .

**Remark 6** (Computational Complexity). *Primal-dual interior-point methods for SDPs have a worst-case complexity estimate of  $\mathcal{O}(m^{2.75} L^{1.5})$ , where  $m$  is the number of variables (a function of  $N, n_x, n_u, n_z$ ) and  $L$  is the number of constraints [21].\* Solving the SCAs involves iteratively obtaining a converging solution to the BMIs, and hence it is difficult to obtain an upper bound on the number of iterations and thus perform any comparison of SCAs with the MISDP (41). But the worst-case complexity of (41) is  $\mathcal{O}(2^N m^{2.75} L^{1.5})$  (notice the exponential factor). As for the SDP relaxation,*

\*In various problems arising in control systems studies, it is shown that the complexity estimate is closer to  $\mathcal{O}(m^{2.1} L^{1.2})$  which is significantly smaller than the worst-case estimate  $\mathcal{O}(m^{2.75} L^{1.5})$  [21].

the computational complexity is only that of an SDP, hence it scales better than MISDPs or the SCAs.

**Remark 7.** Replacing the integrality constraint on  $\pi$  with the box constraint in (41) yields an SDP that can be solved using classical SDP solvers. To obtain the binary actuator selection, Algorithm 3 can be implemented. This can significantly reduce the computational time.

### VIII. SAA SELECTION VIA SUBOPTIMAL ROUTINES

Another alternative to the successive convex approximations, the semidefinite relaxations, and the mixed-integer optimization approach described in the previous sections is a combinatorial greedy algorithms. Greedy algorithms for actuator selection are studied in [44] for Gramian-based metrics and in [45] for optimal feedback control performance metrics in discrete time. We briefly summarize and extend this approach. The greedy algorithm can be viewed as a general combinatorial gradient descent that is applicable in a much broader array of settings than specific Gramian or optimal control metrics. In particular, greedy algorithms can be used to obtain suboptimal, but often good, selections of SaAs in CPSs.

The selection problems described above can be formulated as (combinatorial) set function optimization problems. We discuss formulations for actuator selection; sensor selection can be obtained analogously. For any given actuator selection  $\pi$ , let  $\Pi_s = \{i \in \{1, \dots, N\} \mid \pi_i = 1\}$  denote the selected actuator subset; note that  $\Pi_s \subseteq \{1, \dots, N\}$ . For any of the problems in Table VII, one can associate an objective or constraint function that is being optimized or satisfied and depends on the selected actuator subset  $\Pi_s$ . We will discuss some specific examples for concreteness subsequently. For now, let  $f : 2^{\{1, \dots, N\}} \rightarrow \mathbb{R}$  be a set function that maps a given actuator selection to a control objective function value, and let  $g : 2^{\{1, \dots, N\}} \rightarrow \mathbb{R}$  and  $h : 2^{\{1, \dots, N\}} \rightarrow \mathbb{R}$  be set functions that map a given actuator selection to control constraint function values. Then the actuator selection problem is the constrained set function optimization problem

$$\underset{\Pi_s \subseteq \{1, \dots, N\}}{\text{minimize}} \quad f(\Pi_s) \quad (42a)$$

$$\text{subject to} \quad h(\Pi_s) = 0 \quad (42b)$$

$$g(\Pi_s) \leq 0. \quad (42c)$$

A common heuristic for solving this problem is the greedy algorithm shown in Algorithm 1, which simply adds at each step the actuator that provides the best marginal performance gain, until the constraints are satisfied. Note that the control objective function values associated with the problems in Table VII are monotone in actuator subsets, since having more actuators can only improve the possible control performance. In addition, Algorithm 1 returns a feasible, though possibly suboptimal solution.

One common special case is  $h(\Pi_s) = |\Pi_s| - k$  for some fixed integer  $k$  and  $g$ . This corresponds to a cardinality constrained set function optimization problem, in which a fixed number  $k$  of actuators is added to optimize the control objective function  $f$ .

---

**Algorithm 1** A greedy heuristic for set function optimization.

---

```

 $\Pi_s \leftarrow \emptyset$ 
while  $g(\Pi_s) > 0$  or  $h(\Pi_s) \neq 0$  do
   $e^* = \underset{e \in \{1, \dots, N\} \setminus \Pi_s}{\text{argmin}} \quad f(\Pi_s \cup \{e\})$ 
   $\Pi_s \leftarrow \Pi_s \cup \{e^*\}$ 
end while
 $\Pi_s^* \leftarrow \Pi_s$ 

```

---

We now explain how each of the SaA selection problems in Tables VII and VIII in Appendix E, and combinations thereof, can be cast as a set function optimization problem as described above. For the stabilizability problem in the first row of Table I, we let  $f$  be the set function that maps any actuator subset to the number of unstable and uncontrollable modes. We then define the constraint function  $h = f$ , and the constraint function  $g$  is not used. Then Algorithm 1 can be directly applied and works as follows: at each iteration the actuator that gives the largest marginal reduction of the number of unstable and uncontrollable modes is added, and this is repeated until an actuator subset that results in zero unstable and uncontrollable modes is found. Similar formulations can be obtained for the output feedback control and nonlinear stabilizability problems by defining analogous set functions that map actuator subsets to the number of unstable modes that cannot be affected by output feedback or by state feedback in the presence of the nonlinearity. Furthermore, for the robust control and LQR problems, one can also define set functions that map an actuator subset to the optimal value of the corresponding SDPs listed in Tables VII and VIII, and then directly apply Algorithm 1.

It is also straightforward to handle combinations of the actuator selection problems in Table VII with Algorithm 1. For example, we can optimize robust control performance subject to a stabilizability constraint by taking the set function  $f$  to be the optimal value of the robust control SDP, and  $h$  to be the number of unstable and uncontrollable modes. Moreover, we could put an additional constraint on the LQR control performance by defining  $g$  to be the difference between the optimal value of the LQR control SDP and some desired LQR performance level. Algorithm 1 would then directly apply to find an actuator subset that optimizes robust control performance while providing stabilizability and a given level of LQR control performance. Similar formulations can be easily obtained for all sensor selection problems listed in Table VIII.

Although the greedy algorithm does not necessarily produce an optimal subset of sensors and actuators or even one with a sub-optimality guarantee in general, it can produce highly effective subsets in practice and can be applied to a much broader range of control and estimation problems than has been previously considered in the literature. However, the greedy algorithms that have been developed in the literature solve simpler problems at each iteration of the greedy algorithm. When SDPs are considered as a general framework, each individual iteration of the greedy heuristic solves an SDP. This implies that greedy algorithms might not be more effi-

TABLE I

THE VALUE FOR THE OBJECTIVE FUNCTION  $\zeta + \sum_i^N \pi_i$  FOR DIFFERENT ACTUATOR SELECTION METHODS AND VARIOUS NUMBER OF NODES  $N$ . THIS TEST CORRESPONDS TO THE MASS-SPRING SYSTEM.

$N$	$B_M$ (Big-M)	$\tilde{L}$ (SDP-R)	$\hat{L}^{(1)}$ (SCA-1)	$\hat{L}^{(2)}$ (SCA-2)
5	5.000012	1.000011	1.24	1.24
10	10.000012	2.000011	2.28	2.27
15	15.000012	3.000011	3.29	3.29
20	20.000012	5.000011	5.37	5.36
25	25.000012	6.000011	6.37	6.36
30	30.000012	7.000011	7.36	7.35
35	35.000012	8.000011	8.36	8.35
40	40.000012	10.000011	10.39	10.38
45	45.000012	11.000011	11.39	11.38
50	50.000012	12.000011	12.38	12.37

cient than the alternatives developed in the previous sections (SDP-R, SCAs, and Big-M). A further limitation of greedy algorithms occurs during the first iteration when no single element yields a feasible solution to the studied SDP. In this case it is not obvious which sensor or actuator to select since in some sense all yield infeasible solutions. Further development is required in such cases to refine the evaluation of each sensor or actuator. This limitation is experienced in the numerical tests, which are presented in the next section.

## IX. NUMERICAL TESTS

In this work, we present five different methods to solve the actuator selection with a focus on the  $\mathcal{L}_\infty$  control problems in specific. We also showed that other control and estimation formulations can be formulated in the same fashion. To recap, the three methods rely on relaxing the integrality constraints. The first method is an SDP relaxation providing a lower bound to the optimal solution of the problem with BMIs. The second and third methods are successive convex approximations producing an upper bound on the BMI solutions. If these lower and upper bounds are close to each other, then the optimal solution to the problem with BMIs can be recovered. This is followed by a slicing algorithm that returns an upper bound on the optimization problem with MIBMIs (Appendix D). The fourth method describes a MISDP formulation that leverages disjunctive programming and the Big-M method. Finally, sub-optimal greedy routines are provided.

This section presents a thorough computational comparison of the developed methods. All the simulations are performed using MATLAB R2016b running on 64-bit Windows 10 with Intel Core i7-6700 CPU with base frequency of 3.4GHz and 16 GB of RAM. Yalmip [46] is used as a modeling language whereas SeDuMi [47] is used as the SDP solver for most methods, except the Big-M method, which uses Yalmip's internal branch-and-bound solver.

### A. Simulated Dynamic Systems

We use two different plants which are the mass-spring system and the network of unstable nodes [48]. We consider these plants for two reasons. First, both systems consist of user-defined network size, and second, they have different characteristics in terms of controllability. The mass spring system is controllable for  $N \leq 20$ , whereas the network of unstable nodes is uncontrollable for all  $N$ . Both systems are stabilizable, which is an assumption that is needed for the closed loop linear system without unknown inputs.

In general, the state space of these two systems is of the form  $\dot{\mathbf{x}}(t) = \mathbf{A}\mathbf{x}(t) + \mathbf{B}_u\mathbf{u}(t) + \mathbf{B}_w\mathbf{w}(t)$ ,  $\mathbf{z}(t) = \mathbf{C}\mathbf{x}(t)$ . The state-space matrices of mass-spring system are given as  $\mathbf{A} = \begin{bmatrix} \mathbf{O}_N & \mathbf{I}_N \\ \mathbf{T}_N & \mathbf{O}_N \end{bmatrix}$ ,  $\mathbf{B}_u = \mathbf{B}_w = \begin{bmatrix} \mathbf{O}_N \\ \mathbf{I}_N \end{bmatrix}$ , where  $\mathbf{T}_N$  is a tridiagonal symmetric Toeplitz matrix [48]. The network of unstable nodes has the following structure

$$\dot{\mathbf{x}}_i(t) = \begin{bmatrix} 1 & 1 \\ 1 & 2 \end{bmatrix} \mathbf{x}_i(t) + \sum_{i \neq j} e^{-\alpha(i,j)} \mathbf{x}_j(t) + \begin{bmatrix} 0 \\ 1 \end{bmatrix} (\mathbf{u}_i(t) + \mathbf{w}_i(t)),$$

where the coupling between nodes  $i$  and  $j$  is determined by the Euclidean distance  $\alpha(i, j)$ . These distances are unique for every  $N$  and randomly generated inside a box of size  $N/5$ .

### B. Parameters, Constraints, and Setup

We consider  $N = 5, 10, \dots, 50$  for the two systems. We also use the following specific parameters and constraints.

- The constraint  $\mathbf{H}\boldsymbol{\pi} \leq \mathbf{h}$  is represented as  $\sum_{i=1}^N \pi_i \geq \lfloor N/4 \rfloor$ , where  $\lfloor \cdot \rfloor$  denotes the floor function. We also set  $\boldsymbol{\alpha}_\pi^\top = [1, \dots, 1]$ , that is all actuators have equal weight.
- For SCA-1 and SCA-2, to obtain  $\mathbf{S}_0$ ,  $\zeta_0$ , and  $\mathbf{Z}_0$ , we initialize by assuming that  $\boldsymbol{\Pi}_0 = \mathbf{I}_{n_u}$ , and subsequently solving the  $\mathcal{L}_\infty$  SDP with  $\mathbf{S}_0 \succeq \epsilon_1 \mathbf{I}$  and  $\zeta_0 \geq \epsilon_1$ , where  $\epsilon_1 = 0.1$ . The regularization parameter is set to  $\rho = 0.001$ . We use the value of 0.1 as the tolerance and restrict the number of iterations to 50. Other parameters that are used are  $c_1 = 10^{-3}$ ,  $c_2 = 10^5$ , and  $c_3 = -10^{-3}$ .
- The Big-M method constant is chosen as  $M = 10^7$ . For smaller values of  $M$ , the branch-and-bound solver on Yalmip [43] failed to return feasible solutions.

### C. Comparing the Five Methods and Relevance to the Theory

1) *Results for the Mass-Spring System:* Here, we show two sets of results. First, Table I shows the performance of the first four methods (Big-M, SDP-R, SCA-1, SCA-2) before applying Slicing Algorithm 3. Table I shows the value for the objective function of each individual method. The first observation is that the objective values from (17) are lower than those of obtained from (30) and (38), i.e.,  $\tilde{L} \leq \hat{L}^{(1)\text{or}(2)}$ . This fact follows our proposed methods: Solving (17) yields lower bounds and solving (30) or (38) yields upper bounds on the relaxed problem with BMIs (all of these bounds are lower bounds on the optimal solution  $f^*$ ). This observation corroborates the propositions in Sections V and VI. Looking at the objective values of the SDP-R and SCAs in Table I, it can be seen that the values are not very different. This implies that the solution to the nonconvex problem (5) with relaxed integrality constraints is between these values, and hence the two approximations and relaxations are able to generate good estimates for the solution of the BMIs; see Remark 5. This result is true for different values of  $N$ . Hence, these methods give reasonable bounds on  $L$ .

The second set of results is presented in Table II which depicts the results after applying the slicing algorithm. Note

<sup>†</sup>As mentioned in Section VIII, a limitation of greedy algorithms occurs during the first few iterations when no single element yields a feasible solution to the studied SDP, which then yields a rather large performance index in subsequent iterations as seen in the table.

TABLE II

FINAL RESULTS AFTER RUNNING ALGORITHM 3 TO RECOVER THE BINARY ACTUATOR SELECTION.. THE ‘—’ SYMBOL DENOTES NUMERICAL ISSUES, AND THE BOLDFACED NUMBERS DESCRIBE THE METHOD THAT OUTPERFORMED OTHER METHODS. FOR THE MAJORITY OF THE CASES, THE METHODS DEVELOPED IN THIS PAPER OUTPERFORM THE BIG-M METHOD IN TERMS OF THE OBJECTIVE FUNCTION VALUE AND COMPUTATIONAL TIME.

$N$	Performance Index $\sqrt{\zeta}$				Total Activated Actuators $\sum_i^N \pi_i$				$f_{\text{final}} = \zeta + \sum_i \pi_i$				$\max(\text{eig}(\mathbf{A} - \mathbf{B}_u \mathbf{\Pi} \mathbf{K}))$			
	Big-M	SDP-R	SCA-1	SCA-2	Big-M	SDP-R	SCA-1	SCA-2	Big-M	SDP-R	SCA-1	SCA-2	Big-M	SDP-R	SCA-1	SCA-2
5	0.0034	—	—	—	5	2	1	1	<b>5</b>	—	—	—	-1.2	-1.1	-1.1	-1.1
10	0.0034	3.14	3.14	3.14	10	2	2	2	<b>10</b>	11.9	11.9	11.9	-1.2	-1.1	-1.1	-1.1
15	0.0035	3.07	3.17	3.17	15	4	3	3	15	13.5	<b>13.0</b>	<b>13.0</b>	-1.2	-1.1	-1.1	-1.1
20	0.0035	—	3.10	3.10	20	5	5	5	20	—	<b>14.6</b>	<b>14.6</b>	-1.2	-1.1	-1.1	-1.1
25	0.0034	2.83	2.87	2.87	25	6	6	6	25	<b>14.0</b>	14.2	14.2	-1.2	-1.3	-1.2	-1.2
30	0.0035	3.12	3.04	2.95	30	8	9	10	30	<b>17.7</b>	18.3	18.7	-1.2	-1.1	-1.1	-1.1
35	0.0034	3.18	2.97	2.97	35	8	14	14	35	<b>18.1</b>	22.8	22.8	-1.2	-1.1	-1.2	-1.1
40	0.0035	3.01	2.98	2.96	40	15	16	17	40	<b>24.1</b>	24.9	25.7	-1.2	-1.1	-1.1	-1.1
45	0.0034	2.84	3.00	2.73	45	13	18	19	45	<b>21.1</b>	27.0	26.4	-1.2	-1.2	-1.1	-1.2
50	0.0034	2.78	3.00	2.71	50	21	19	22	50	28.7	<b>28.0</b>	29.3	-1.2	-1.1	-1.2	-1.3

TABLE III

NUMERICAL RESULTS BASED ON GREEDY ALGORITHM FOR THE MASS-SPRING SYSTEM ( $\tilde{\mathbf{A}} = \mathbf{A} - \mathbf{B}_u \mathbf{\Pi} \mathbf{K}$ ).

$N$	$\zeta + \sum_i^N \pi_i$	$\sqrt{\zeta}$	$\sum_i^N \pi_i$	$\max(\text{eig}(\tilde{\mathbf{A}}))$	$\Delta t$ (s)
5	816.0	28.5	2	-1.50	19.2
10	56425.8	237.5 <sup>†</sup>	3	-1.41	13.0
15	89924.2	299.9	4	-1.33	50.0
20	2259.0	47.4	8	-1.28	329.0
25	103865.8	322.3	8	-1.28	861.6
30	101781.6	319.0	11	-1.31	4157.9

that Algorithm 3 is not applied to the Big-M solutions, as these solutions are binary—this is the reason why the Big-M figures are identical in Tables I and II. Table II presents the performance index,  $\sqrt{\zeta}$ , the total activated actuators  $\sum_i \pi_i$ , the objective function value  $f_{\text{final}}$ , and the closed-loop system eigenvalues.

The numbers in boldface in the  $f_{\text{final}}$  column illustrate the method with the smaller objective function value. While Big-M yielded the smallest  $f_{\text{final}}$  for  $N = 5, 10$ , the other methods (SDP-R, SCA-1, SCA-2) yield significantly superior objective values for the mass-spring system and the network with unstable nodes. This, however, does not come at the cost of compromising the closed-loop system stability: the spectral abscissa of the system did not worsen when fewer actuators are activated. The results also show the trade-off between the robustness index and the number of activated actuators. It is noteworthy to mention that adding only few extra actuators can significantly improve the corresponding performance index. Finally, the Big-M method needed tuning: for values of  $M < 10^7$ , the solver fails to return a feasible solution. In addition, for much larger values of  $M$ , the solver suffers from expected numerical problems. The authors in [41] discuss alternative optimization methods to solve mixed-integer semidefinite programs.

2) *Discussion on Greedy Algorithms:* Greedy Algorithm 1 is implemented. The inequality constraint in the set function optimization is  $\mathbf{H}\boldsymbol{\pi} \leq \mathbf{h}$ . Table III shows the objective function values and the computational time for different network size, in addition to the robustness index and closed loop system eigenvalues. The greedy algorithm returns a small number of actuators, but at the expense of large  $\zeta$ . The algorithm failed to converge for  $N = 35, \dots, 50$  after three days of computations, and hence terminated. Greedy algorithms provide good alternatives to problems where individual sub-problem with fixed actuator selection can be executed rapidly. In the case of SDPs, greedy algorithms do not outperform any

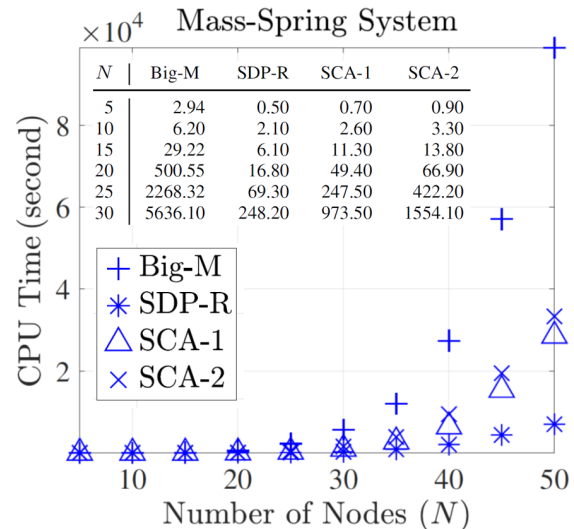


Fig. 1. CPU time for the different methods and various number of nodes  $N$ . The computational time for  $N = 5, \dots, 30$  is difficult to show on the same figure, so the results are tabulated inside the figure.

of the first four methods in terms of computational time or performance since sub-problems in each iteration of the greedy algorithm requires solving an SDP. This further signifies the value of the proposed SDP relaxations and SCAs.

3) *Computational Time:* Fig. 1 shows the CPU time for the first four methods. As discussed in Remark 6, SDP-R is expected to be computationally more efficient than the other methods—this can be observed from Fig. 1. Since SCA-1 includes a smaller number of constraints and variables than SCA-2 (see Section VI-C), the former requires less computational time. The Big-M method is the slowest for the mass-spring system, although the solver terminates at 300 iterations of the branch-and-bound routine. In many instances, the solver terminated while the gap percentage between the lower and upper bounds was still greater than 10%.

4) *Results for System with Unstable Nodes:* Similar to the results corresponding to the mass-spring system, Tables IV, V, and VI, we show the results for the system with unstable nodes for different values of  $N$  (and for the five methods). The results are consistent with the findings in the previous tests on the mass-spring system, with the difference that the Big-M method occasionally requires less computational time than the SCAs; see Fig. 2 and the table within. However, the SCAs and the SDP-R provides in general a better overall objective function

TABLE IV  
THE VALUE FOR THE OBJECTIVE FUNCTION  $\zeta + \sum_i^N \pi_i$  FOR DIFFERENT ACTUATOR SELECTION METHODS AND VARIOUS NUMBER OF NODES  $N$ . THIS TEST CORRESPONDS TO THE SYSTEM WITH UNSTABLE NODES.

$N$	$B_M$ (Big-M)	$\tilde{L}$ (SDP-R)	$\hat{L}^{(1)}$ (SCA-1)	$\hat{L}^{(2)}$ (SCA-2)
5	5.00008	1.00008	1.05055	1.05039
10	10.00014	2.00014	2.09409	2.09392
15	15.00016	3.00016	3.09680	3.09610
20	20.00015	5.00015	5.10562	5.10516
25	25.00010	6.00010	6.06461	6.06441
30	30.00022	7.00022	7.13780	7.14858
35	35.00014	8.00013	8.07569	8.07613
40	40.00014	10.00014	10.09324	10.09346
45	45.00013	11.00013	11.08279	11.08311
50	50.00010	12.00010	12.06388	12.06371

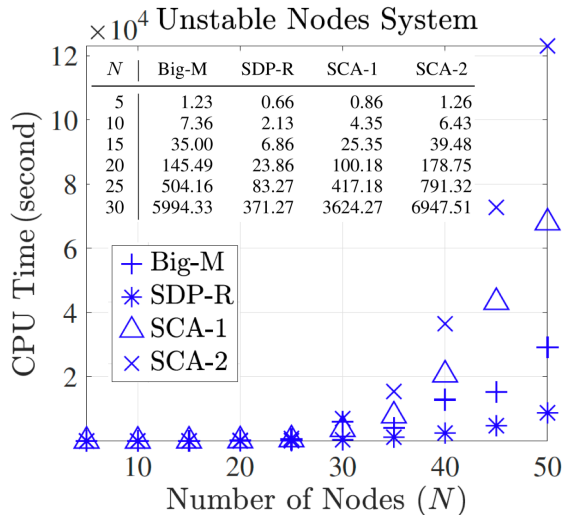


Fig. 2. CPU time for the different methods with various values for the number of nodes  $N$ . These results correspond to the system with unstable nodes.

value for larger system sizes. More numerical experiments are needed to compare the computational effectiveness of the Big-M method and the SCAs.

5) *Final Remark*: In this paper, we only utilize the  $\mathcal{L}_\infty$  control problem with actuator selection to exemplify how the proposed relaxations and approximations can provide insights into the solution of a challenging combinatorial optimization problem. We leave the derivations of other sensor and actuator selection problems with different metrics and nonlinear dynamics as an exercise for the interested reader, while emphasizing that all other metrics and CPS dynamics in Tables VII and VIII with SaA selection follow the same developed methods.

## X. SUMMARY AND FUTURE WORK

This paper puts a framework to solve SaA selection problems for uncertain CPSs with various control and estimation metrics. Given the widely popular SDP formulations of various control/estimation problems (without SaA selection), we present various techniques that aim to recover, approximate, or bound the optimal solution to the combinatorial SaA selection problem via convex programming. While the majority of prior art focuses on specific metrics or dynamics, the objective of this paper is to present a unifying framework that streamlines

the problem of time-varying SaA selection in uncertain and potentially nonlinear CPSs.

We plan to study the following related research problems in future work. (1) Simultaneous SaA selection for output feedback control problems. This problem produces more complex integer programming problems than MIBMIs. (2) Applications to selection of distributed generation in electric power networks with frequency-performance guarantees. (3) Customized branch-and-bound methods.

## REFERENCES

- [1] Y.-Y. Liu, J.-J. Slotine, and A.-L. Barabási, “Controllability of complex networks,” *Nature*, vol. 473, no. 7346, pp. 167–173, 2011.
- [2] T. Nepusz and T. Vicsek, “Controlling edge dynamics in complex networks,” *Nature Physics*, vol. 8, no. 7, pp. 568–573, 2012.
- [3] J. Ruths and D. Ruths, “Control profiles of complex networks,” *Science*, vol. 343, no. 6177, pp. 1373–1376, 2014.
- [4] A. Olshevsky, “Minimal controllability problems,” *IEEE Transactions on Control of Network Systems*, vol. 1, no. 3, pp. 249–258, 2014.
- [5] S. Pequito, S. Kar, and A. Aguiar, “A framework for structural input/output and control configuration selection in large-scale systems,” *IEEE Transactions on Automatic Control*, vol. 61, no. 2, pp. 303–318, 2016.
- [6] F. Pasqualetti, S. Zampieri, and F. Bullo, “Controllability metrics, limitations and algorithms for complex networks,” *Control of Network Systems, IEEE Transactions on*, vol. 1, no. 1, pp. 40–52, 2014.
- [7] T. H. Summers and J. Lygeros, “Optimal sensor and actuator placement in complex dynamical networks,” *IFAC Proceedings Volumes*, vol. 47, no. 3, pp. 3784–3789, 2014.
- [8] T. Summers, F. Cortesi, and J. Lygeros, “On submodularity and controllability in complex dynamical networks,” *IEEE Transactions on Control of Network Systems*, vol. 3, no. 1, pp. 91–101, 2016.
- [9] V. Tzoumas, M. A. Rahimian, G. Pappas, and A. Jadbabaie, “Minimal actuator placement with bounds on control effort,” *IEEE Transactions on Control of Network Systems*, vol. 3, no. 1, pp. 67–78, 2016.
- [10] G. Yan, G. Tsekenis, B. Barzel, J.-J. Slotine, Y.-Y. Liu, and A.-L. Barabási, “Spectrum of controlling and observing complex networks,” *Nature Physics*, vol. 11, pp. 779–786, 2015.
- [11] Y. Zhao, F. Pasqualetti, and J. Cortés, “Scheduling of control nodes for improved network controllability,” in *IEEE Conference on Decision and Control*. IEEE, 2016, pp. 1859–1864.
- [12] E. Nozari, F. Pasqualetti, and J. Cortes, “Time-varying actuator scheduling in complex networks,” *arXiv preprint arXiv:1611.06485*, 2016.
- [13] P. V. Chanekar, N. Chopra, and S. Azarm, “Optimal actuator placement for linear systems with limited number of actuators,” in *2017 American Control Conference (ACC)*, May 2017, pp. 334–339.
- [14] B. Polyak, M. Khlebnikov, and P. Shcherbakov, “An lmi approach to structured sparse feedback design in linear control systems,” in *European Control Conference*, July 2013, pp. 833–838.
- [15] N. K. Dhingra, M. R. Jovanović, and Z.-Q. Luo, “An admm algorithm for optimal sensor and actuator selection,” in *IEEE Conference on Decision and Control*. IEEE, 2014, pp. 4039–4044.
- [16] A. Argha, S. W. Su, and A. Savkin, “Optimal actuator/sensor selection through dynamic output feedback,” in *2016 IEEE 55th Conference on Decision and Control (CDC)*, Dec 2016, pp. 3624–3629.
- [17] T. Summers, “Actuator placement in networks using optimal control performance metrics,” in *IEEE Conference on Decision and Control*. IEEE, 2016, pp. 2703–2708.
- [18] T. Summers and J. Ruths, “Performance bounds for optimal feedback control in networks,” *arXiv preprint arXiv:1707.04528*, 2017.
- [19] H. Zhang, R. Ayoub, and S. Sundaram, “Sensor selection for kalman filtering of linear dynamical systems: Complexity, limitations and greedy algorithms,” *Automatica*, vol. 78, pp. 202–210, 2017.
- [20] J. A. Taylor, N. Luangsomboon, and D. Fooladivanda, “Allocating sensors and actuators via optimal estimation and control,” *IEEE Transactions on Control Systems Technology*, vol. 25, no. 3, pp. 1060–1067, May 2017.
- [21] S. P. Boyd, L. El Ghaoui, E. Feron, and V. Balakrishnan, *Linear matrix inequalities in system and control theory*. SIAM, 1994, vol. 15.
- [22] A. F. Taha, N. Gatsis, T. Summers, and S. Nugroho, “Actuator selection for cyber-physical systems,” in *2017 American Control Conference (ACC)*, May 2017, pp. 5300–5305.

TABLE V

FINAL RESULTS AFTER RUNNING ALGORITHM 3 TO RECOVER THE BINARY ACTUATOR SELECTION AND THE ACTUAL SYSTEM PERFORMANCE FOR THE SYSTEM WITH UNSTABLE NODES. THE BOLDFACED NUMBERS DESCRIBE THE METHOD THAT OUTPERFORMED OTHER METHODS.

$N$	Performance Index $\sqrt{\zeta}$				Total Activated Actuators $\sum_i^N \pi_i$				$f_{\text{final}} = \zeta + \sum_i \pi_i$				$\max(\text{eig}(\mathbf{A} - \mathbf{B}_u \mathbf{\Pi} \mathbf{K}))$			
	Big-M	SDP-R	SCA-1	SCA-2	Big-M	SDP-R	SCA-1	SCA-2	Big-M	SDP-R	SCA-1	SCA-2	Big-M	SDP-R	SCA-1	SCA-2
5	0.009	2.82	2.84	2.84	5	2	2	2	<b>5</b>	10.0	10.0	10.0	-1.2	-1.1	-1.2	-1.2
10	0.012	2.91	2.66	2.66	10	4	4	4	<b>10</b>	12.5	11.1	11.1	-1.2	-1.2	-1.2	-1.2
15	0.012	2.94	2.90	2.90	15	6	7	7	15	<b>14.7</b>	15.4	15.4	-1.2	-1.1	-1.2	-1.2
20	0.012	2.67	2.88	2.88	20	9	9	9	20	<b>16.1</b>	17.3	17.3	-1.3	-1.3	-1.2	-1.2
25	0.010	2.56	2.90	2.71	25	18	12	12	25	24.5	20.4	<b>19.3</b>	-1.3	-1.2	-1.2	-1.2
30	0.015	2.68	2.71	2.77	30	14	14	14	30	<b>21.2</b>	21.3	21.7	-1.2	-1.2	-1.2	-1.2
35	0.012	2.82	2.72	2.72	35	16	15	15	35	24.0	22.4	<b>22.4</b>	-1.2	-1.2	-1.2	-1.2
40	0.012	2.65	2.69	2.73	40	21	18	18	40	28.0	<b>25.2</b>	25.5	-1.2	-1.2	-1.2	-1.2
45	0.011	2.63	2.75	2.71	45	29	18	19	45	35.9	<b>25.5</b>	26.4	-1.2	-1.2	-1.3	-1.2
50	0.010	2.72	2.85	2.69	50	24	24	23	50	31.4	32.1	<b>30.2</b>	-1.2	-1.2	-1.2	-1.2

TABLE VI

NUMERICAL RESULTS BASED ON GREEDY ALGORITHM FOR THE SYSTEM WITH UNSTABLE NODES ( $\tilde{\mathbf{A}} = \mathbf{A} - \mathbf{B}_u \mathbf{\Pi} \mathbf{K}$ ).

$N$	$\zeta + \sum_i^N \pi_i$	$\sqrt{\zeta}$	$\sum_i^N \pi_i$	$\max(\text{eig}(\tilde{\mathbf{A}}))$	$\Delta t$ (s)
5	745.0	27.2	3	-1.84	11.2
10	15841.0	125.8	5	-1.75	29.6
15	24545.2	156.6	8	-1.56	127.5
20	215516.3	464.2	10	-1.77	474.8
25	158632.4	398.3	14	-1.48	2088.4
30	217274.3	466.1	18	-1.46	9359.9

- [23] D. G. Eliades, "Fault diagnosis and security monitoring in water distribution systems," Ph.D. dissertation, University of Cyprus, Faculty of Engineering, 2011.
- [24] J. G. VanAntwerp and R. D. Braatz, "A tutorial on linear and bilinear matrix inequalities," *Journal of Process Control*, vol. 10, no. 4, pp. 363–385, 2000.
- [25] Y. T. Lee, A. Sidford, and S. C.-w. Wong, "A faster cutting plane method and its implications for combinatorial and convex optimization," in *Foundations of Computer Science (FOCS), 2015 IEEE 56th Annual Symposium on*. IEEE, 2015, pp. 1049–1065.
- [26] J. van Apeldoorn, A. Gilyén, S. Gribbling, and R. de Wolf, "Quantum sdp-solvers: Better upper and lower bounds," *arXiv preprint arXiv:1705.01843*, 2017.
- [27] A. A. Ahmadi and G. Hall, "Sum of squares basis pursuit with linear and second order cone programming," 2015.
- [28] I. Dunning, J. Huchette, and M. Lubin, "Jump: A modeling language for mathematical optimization," *SIAM Review*, vol. 59, no. 2, pp. 295–320, 2017.
- [29] I. E. Grossmann, "Review of nonlinear mixed-integer and disjunctive programming techniques," *Optimization and engineering*, vol. 3, no. 3, pp. 227–252, 2002.
- [30] T. Pancake, M. Corless, and M. Brockman, "Analysis and control of polytopic uncertain/nonlinear systems in the presence of bounded disturbance inputs," in *American Control Conference, 2000. Proceedings of the 2000*, vol. 1, no. 6. IEEE, 2000, pp. 159–163.
- [31] M. Johansson and A. Rantzer, "Computation of piecewise quadratic lyapunov functions for hybrid systems," *IEEE transactions on automatic control*, vol. 43, no. 4, pp. 555–559, 1998.
- [32] A. Shapiro, "First and second order analysis of nonlinear semidefinite programs," *Mathematical Programming*, vol. 77, no. 1, pp. 301–320, 1997.
- [33] A. Shapiro and K. Scheinberg, "Duality and optimality conditions," in *Handbook of Semidefinite Programming*, H. Wolkowicz, R. Saigal, and L. Vandenberghe, Eds. Springer, 2000, ch. 4, pp. 67–110.
- [34] B. Recht, M. Fazel, and P. A. Parrilo, "Guaranteed minimum-rank solutions of linear matrix equations via nuclear norm minimization," *SIAM review*, vol. 52, no. 3, pp. 471–501, 2010.
- [35] R. A. Horn and C. R. Johnson, *Matrix Analysis*, 2nd ed. New York, NY: Cambridge University Press, 2013.
- [36] Q. T. Dinh, S. Gumussoy, W. Michiels, and M. Diehl, "Combining convex-concave decompositions and linearization approaches for solving bmis, with application to static output feedback," *IEEE Transactions on Automatic Control*, vol. 57, no. 6, pp. 1377–1390, 2012.
- [37] S. Boyd and L. Vandenberghe, *Convex optimization*. Cambridge university press, 2004.
- [38] D. Lee and J. Hu, "A sequential parametric convex approximation method for solving bilinear matrix inequalities," in *2016 IEEE 55th Conference on Decision and Control (CDC)*, Dec 2016, pp. 1965–1970.
- [39] K. B. Petersen, M. S. Pedersen *et al.*, "The matrix cookbook," *Technical University of Denmark*, vol. 7, p. 15, 2008.
- [40] B. R. Marks and G. P. Wright, "A general inner approximation algorithm for nonconvex mathematical programs," *Operations Research*, vol. 26, no. 4, pp. 681–683, 1978.
- [41] F. W. Kong, D. Kuhn, and B. Rustem, "A cutting-plane method for mixed-logical semidefinite programs with an application to multi-vehicle robust path planning," in *49th IEEE Conference on Decision and Control (CDC)*, Dec 2010, pp. 1360–1365.
- [42] "Mixed-integer support in CVX 2.0," CVX Research, 2012 Aug. 31. [Online]. Available: <http://cvxr.com/news/2012/08/midcp/>
- [43] "Integer programming," YALMIP Wiki, Sept. 1 2015. [Online]. Available: <http://users.isy.liu.se/johanl/yalmip/pmwiki.php?n=Tutorials.IntegerProgramming>
- [44] T. H. Summers, F. L. Cortesi, and J. Lygeros, "On submodularity and controllability in complex dynamical networks," *IEEE Transactions on Control of Network Systems*, vol. 3, no. 1, pp. 91–101, March 2016.
- [45] T. Summers, "Actuator placement in networks using optimal control performance metrics," in *to appear, IEEE Conference on Decision and Control*. IEEE, 2016.
- [46] J. Löfberg, "Yalmip: A toolbox for modeling and optimization in matlab," in *Proc. IEEE Int. Symp. Computer Aided Control Systems Design*. IEEE, 2004, pp. 284–289.
- [47] Y. Labit, D. Peaucelle, and D. Henrion, "Sedumi interface 1.02: a tool for solving lmi problems with sedumi," in *Computer Aided Control System Design, 2002. Proceedings. 2002 IEEE International Symposium on*. IEEE, 2002, pp. 272–277.
- [48] [Online]. Available: <http://people.ece.umn.edu/users/mihailo/software/lqrsp/>
- [49] K. Zhou, J. C. Doyle, K. Glover *et al.*, *Robust and optimal control*. Prentice hall New Jersey, 1996, vol. 40.
- [50] C. A. Crusius and A. Trofino, "Sufficient lmi conditions for output feedback control problems," *Automatic Control, IEEE Transactions on*, vol. 44, no. 5, pp. 1053–1057, 1999.
- [51] D. D. Siljak, D. M. Stipanovic, and A. I. Zecevic, "Robust decentralized turbine/governor control using linear matrix inequalities," *IEEE Transactions on Power Systems*, vol. 17, no. 3, pp. 715–722, 2002.
- [52] C. Scherer and S. Weiland, "Linear matrix inequalities in control," *Lecture Notes, Dutch Institute for Systems and Control, Delft, The Netherlands*, vol. 3, 2000.
- [53] A. Chakrabarty, M. J. Corless, G. T. Buzzard, S. H. Zak, and A. E. Rundell, "State and unknown input observers for nonlinear systems with bounded exogenous inputs," *Proc. of the 2016 American Control Conference*, pp. 103–108.
- [54] W. Zhang, H. Su, H. Wang, and Z. Han, "Full-order and reduced-order observers for one-sided lipschitz nonlinear systems using riccati equations," *Communications in Nonlinear Science and Numerical Simulation*, vol. 17, no. 12, pp. 4968–4977, 2012.
- [55] R. Rajamani, "Observers for lipschitz nonlinear systems," *IEEE transactions on Automatic Control*, vol. 43, no. 3, pp. 397–401, 1998.

APPENDIX A  
NOTATION

Italicized, boldface upper and lower case characters represent matrices and column vectors— $a$  is a scalar,  $\mathbf{a}$  is a vector, and  $\mathbf{A}$  is a matrix. Matrix  $\mathbf{I}_n$  is the identity square matrix of size  $n$ , and vector  $\mathbf{1}_n$  is a vector of ones of size  $n$ ;  $\mathbf{O}_{m \times n}$  defines a zero matrix of size  $m \times n$ .  $\mathbb{S}^n$  denotes the set of symmetric matrices of size  $n$ ;  $\mathbb{S}_+^n$  and  $\mathbb{S}_{++}^n$  are the sets of symmetric positive semidefinite and positive definite matrices. By definition, and unless otherwise specified, we assume that all matrices  $\mathbf{S}$  and  $\mathbf{P}$  in the paper are positive definite, i.e.,  $\mathbf{S}, \mathbf{P} \in \mathbb{S}_{++}^n$ .  $\|\mathbf{A}\|$ ,  $\|\mathbf{A}\|_F$ ,  $\|\mathbf{A}\|_* = \sqrt{\left(\sum_{i=1}^m \sum_{j=1}^n |a_{ij}|^2\right)}$  and  $\|\mathbf{A}\|_*$  denote the spectral, Frobenius, and nuclear norms of  $\mathbf{A}$ . The symbol  $\text{diag}(\mathbf{a})$  denotes a diagonal matrix whose diagonal entries are given by the vector  $\mathbf{a}$ ;  $\text{diag}(\mathbf{A})$  forms a column vector by extracting the diagonal entries of  $\mathbf{A}$ . The symbol  $\Lambda(\mathbf{A})$  denotes the set of complex eigenvalues of a matrix  $\mathbf{A}$ .

APPENDIX B

ACTUATOR SELECTION: THE LOGISTIC CONSTRAINTS

The constraint  $\mathbf{H}\boldsymbol{\pi} \leq \mathbf{h}$  couples the selected actuators across time periods, and is a linear logistic constraint that includes the following scenarios.

- Activation and deactivation of SaAs in a specific time-period  $j$ . For example, if actuator  $i$  cannot be selected at period  $j$ , we set  $\pi_i^j \leq 0$ .
- If actuator  $k$  is allowed to be selected only after actuator  $i$  is selected at period  $j$ , we set  $\pi_k^{j+1} \leq \pi_i^j$ , for  $j = 1, \dots, T_f$ .
- If actuator  $k$  must be deselected after actuator  $i$  is selected at period  $j$ , we set  $\pi_k^{j+1} \leq 1 - \pi_i^j$ , for  $j = 1, \dots, T_f$ .
- Upper and lower bounds on the total number of active SaAs per period can be accounted for.
- Other constraints such as minimal number of required active actuators in a certain region of the CPS, and unit commitment constraints that are obtained from solutions day-ahead planning problems, can be included.

APPENDIX C

SUCCESSIVE CONVEX APPROXIMATION

Algorithm 2 illustrates how the SCAs (30) and (38) can be solved sequentially until a maximum number of iterations (MaxIter) or a stopping criterion defined by a tolerance (tol) are met.

**Algorithm 2** Solving the successive convex approximations.

---

**input:** MaxIterNum, tol,  $k = 0$ ,  $\boldsymbol{\Pi}_0 = \mathbf{I}_{n_u}$   
**while**  $k < \text{MaxIterNum}$  **do**  
  Option 1: Solve (30)  
  Option 2: Solve (38)  
  **if**  $|\hat{L}_k^{(1) \text{ or } (2)} - \hat{L}_{k-1}^{(1) \text{ or } (2)}| < \text{tol}$  **then**  
    **break**  
  **else**  
     $k \leftarrow k + 1$   
  **end if**  
**end while**  
 $\{\mathbf{S}^*, \boldsymbol{\zeta}^*, \mathbf{Z}^*, \boldsymbol{\Pi}^*\} \leftarrow \{\mathbf{S}^k, \boldsymbol{\zeta}^k, \mathbf{Z}^k, \boldsymbol{\Pi}^k\};$

---

APPENDIX D

RECOVERING THE BINARY SELECTION

The solutions obtained from (17), (30), and (38) produce a noninteger solution for the actuator selection problem. Since the objective is to determine a binary selection for the actuators, we present in this section a simple *slicing routine* that returns a binary selection given the solutions to the optimization problems in Sections V and VI.

The slicing routine is presented in Algorithm 3. Since the objective of the  $\mathcal{L}_\infty$  problem is to find a feedback gain  $\mathbf{K} = \mathbf{Z}\mathbf{S}^{-1}$  that renders the closed-loop system stable, the slicing algorithm ensures that the spectrum  $\Lambda(\mathbf{A}_{cl})$  of the closed-loop system matrix  $\mathbf{A}_{cl} = \mathbf{A} - \mathbf{B}_u \boldsymbol{\Pi} \mathbf{K}$  lies on the left-half plane.

The slicing routine takes as an input the real-valued solution to the actuator selection  $\boldsymbol{\Pi}^*$  with  $\pi_i^* \in [0, 1]$ . First, the entries of  $\boldsymbol{\pi}^*$  are sorted in decreasing order, and the minimum  $s$ -actuator selection is obtained such that the logistic constraints  $\mathbf{H}\boldsymbol{\pi} \leq \mathbf{h}$  are satisfied, given that  $\boldsymbol{\pi} \in \{0, 1\}^N$ . This ensures that we start the slicing algorithm from the minimum number of actuators, while still satisfying all of the actuator-related constraints in (6). The algorithm proceeds by activating the  $s$ -highest ranked actuators, followed by solving the  $\mathcal{L}_\infty$  SDP (6a)–(6c) for  $\mathbf{Z}$  and  $\mathbf{S}$ . Then, the maximum real part of the eigenvalues of  $\mathbf{A}_{cl}$ , namely  $\lambda_m$ , is obtained. If  $\lambda_m < 0$ , the algorithm exits returning the actuator selection  $\boldsymbol{\Pi}_s$  and the associated feedback gain.

The algorithm allows the addition of other user-defined requirements, such as a minimum performance index  $\zeta$  or a maximum  $\lambda_m$ , which can guarantee a minimal distance to instability. It can also be generalized to other control or estimation problems. For example, in the case of observer design, the closed loop eigenvalues of  $\mathbf{A} - \mathbf{L}\mathbf{F}\mathbf{C}$  can be used to determine the optimal sensor selection. Other metrics can be similarly included.

**Algorithm 3** A Slicing Algorithm to Recover the Integer Selection from (17), (30), and (38)

---

**input:**  $\boldsymbol{\Pi}^*$  from Algorithm 2, set  $\lambda_m = \infty$   
Sort  $\boldsymbol{\pi}^*$  in a decreasing order  
 $s = \underset{\boldsymbol{\pi} \in \{0, 1\}^N, \mathbf{H}\boldsymbol{\pi} \leq \mathbf{h}}{\text{minimum}} \mathbf{1}_N^\top \boldsymbol{\pi}$   
**while**  $\lambda_m > 0$  **do**  
  Activate the  $s$ -highest ranked actuators in  $\boldsymbol{\pi}$   
  Obtain  $\boldsymbol{\Pi}_s = \text{blkdiag}(\pi_1 \mathbf{I}_{n_{u_1}}, \dots, \pi_N \mathbf{I}_{n_{u_N}})$   
  Given  $\boldsymbol{\Pi} = \boldsymbol{\Pi}_s$ , solve the SDP (6a)–(6c) for  $\mathbf{Z}$  and  $\mathbf{S}$   
   $\lambda_m = \max(\text{real}(\lambda))$  where  $\lambda \in \Lambda(\mathbf{A} - \mathbf{B}_u \boldsymbol{\Pi}_s \mathbf{Z} \mathbf{S}^{-1})$   
   $s \leftarrow s + 1$   
**end while**  
Return the solution  $p_s$  consisting of  $\boldsymbol{\Pi}_s, \mathbf{Z}, \mathbf{S}$ .

---

The actuator selection and associated control law returned by Algorithm 3 yield an upper bound  $U$  to the optimal value of the actuator selection problem (5).

**Proposition 9.** Let  $p_s$  denote the solution obtained from Algorithm 3. It holds that  $f(p_s) = U \geq f^*$ .

*Proof of Proposition 9:* By construction of Algorithm 3, the point  $p_s$  is feasible for (5) since the inequality constraints on the actuator selection are satisfied. Thus, it follows that  $f(p_s) = U \geq f^*$ . ■

## APPENDIX E

## VARIOUS CONTROLLER AND OBSERVER DESIGNS VIA SDP FORMULATIONS FOR DIFFERENT METRICS AND DYNAMICS

TABLE VII

CONTROLLER DESIGN FOR VARIOUS CPS DYNAMICS AND OBJECTIVES VIA SDP FORMULATIONS [21], [49]–[51].

CPS Dynamics, Metrics, & Design Objective	Control Design via SDPs
<i>Stabilization of Linear Systems</i> $\dot{x} = Ax + B_u u$ , Variable: $S$	find $S$ s.t. $AS + SA^\top \preceq B_u B_u^\top$
<i>Robust <math>L_\infty</math> Control of Uncertain Linear Systems</i> $\dot{x} = Ax + B_u u + B_w w$ $z = C_z x + D_{vw} w$ $u = -Kx = -ZS^{-1}x$ , Variables: $Z, S, \zeta$	min $\zeta$ s.t. $\begin{bmatrix} AS + SA^\top - B_u Z - Z^\top B_u^\top + 2\alpha S & B_w \\ & B_w^\top \\ -S & O & SC_z^\top \\ O & -I & D_{wz}^\top \\ C_z S & D_{wz} & -\zeta I \end{bmatrix} \preceq O$ $\zeta > 0$
<i>Stabilization through Output Feedback Control</i> $\dot{x} = Ax + B_u u$ $y = Cx$ $u = -Ky = M^{-1}Ny$ , Variables: $M, N, S$	find $S, N, M$ s.t. $A^\top S + SA - C^\top N^\top B_u^\top - B_u N C \preceq O$ , $B_u M = S B_u$
<i>LQR Control: Minimizing State and Input Energy</i> min $\mathbb{E} \int_{t_0}^{\infty} x(\tau) Q x(\tau) + u(\tau) R u(\tau) d\tau$ s.t. $\dot{x} = Ax + B_u u + w$ , $w \sim \mathcal{N}(0, W)$ $u = -R^{-1} B_u^\top S^{-1} x$ , Variables: $Y, S$	min $\text{trace}(WS^{-1})$ s.t. $\begin{bmatrix} AS + SA^\top + B_u Y + Y^\top B_u^\top & S & Y \\ & S & -Q^{-1} & 0 \\ & Y^\top & 0 & -R^{-1} \end{bmatrix} \preceq O$
<i>Stabilization of Nonlinear Systems</i> $\dot{x} = Ax + B_u u + \phi(x)$ $u = Kx = ZS^{-1}x$ , Variables: $Z, S, \zeta, \kappa_S, \kappa_Z$ $\phi(x)$ bounded by: $\phi^\top(x)\phi(x) \leq \alpha^2 x^\top F^\top F x$	min $\zeta + \kappa_S + \kappa_Z$ s.t. $\begin{bmatrix} AS + SA^\top + B_u Z + Z^\top B_u^\top & I & SF^\top \\ & I & -I & O \\ & FS & O & -\zeta I \end{bmatrix} \prec O$ $\begin{bmatrix} -\kappa_Z I & Z^\top \\ Z & -I \end{bmatrix} \prec O$ , $\begin{bmatrix} Z & I \\ I & \kappa_S I \end{bmatrix} \succ O$ , $\zeta - \frac{1}{\alpha^2} < 0$
<i>Stabilization of Time-Delay Systems</i> $\dot{x} = Ax + B_u u + \sum_{i=1}^L A_i x(t - \tau_i)$ $u = Kx = ZS^{-1}x$ , Variables: $Z, S, S_1, \dots, S_L$	find $Z, S, S_1, \dots, S_L$ s.t. $\begin{bmatrix} AS + SA^\top + B_u Z + Z^\top B_u^\top + \sum_{i=1}^L S_i & A_1 S & \dots & A_L S \\ & SA_1^\top & & -S_1 & \dots & O \\ & \vdots & & \vdots & \ddots & \vdots \\ & SA_L^\top & & O & \dots & -S_L \end{bmatrix} \prec O$

TABLE VIII

ESTIMATORS DESIGN FOR CPSS VIA SDP FORMULATIONS; SEE REFERENCES [52]–[55]. OTHER SIMILAR FORMULATIONS ARE OMITTED FOR BREVITY.

Dynamics & Estimation Objective	Estimator Dynamics	Estimator Design via SDPs
$\dot{\hat{x}} = A\hat{x} + B_u u$ $\hat{y} = C\hat{x} + D_u u$ Variables: $P, Y$	$\dot{\hat{x}} = A\hat{x} + B_u u + L(y - \hat{y})$ $\hat{y} = C\hat{x} + D_u u$ $L = P^{-1}Y$	find $Y$ s.t. $A^\top P + PA - C^\top Y^\top - YC + 2\alpha P \preceq O$
$\dot{x} = Ax + B_u u + B_w w$ $y = Cx + D_u u$ Variables: $P, Y, \mu$	$\dot{\hat{x}} = A\hat{x} + B_u u + L(y - \hat{y})$ $\hat{y} = C\hat{x} + D_u u$ $L = P^{-1}Y$	min $\mu > 0$ s.t. $\begin{bmatrix} A^\top P + PA - \\ C^\top Y^\top - YC - \mu C^\top C & P B_w \\ B_w^\top P & -\mu I \end{bmatrix} \preceq O$ $\mu > 0$
$\dot{x} = Ax + B_u u + B_w w$ $y = Cx + D_u u + D_v v$ Variables: $P, Y, \mu$	$\dot{\hat{x}} = A\hat{x} + B_u u + L(y - \hat{y})$ $\hat{y} = C\hat{x} + D_u u$ $L = P^{-1}Y$	min $\mu$ s.t. $\begin{bmatrix} A^\top P + PA - YC \\ -C^\top Y^\top + \alpha P & P B_w & Y D_v \\ B_w^\top P & -\alpha I & O \\ D_v^\top Y^\top & O & -\alpha I \end{bmatrix} \preceq O$ $P \succeq \mu I$ , $\mu > 0$
$\dot{x} = Ax + B_u u + \phi(x, u)$ $y = Cx + D_u u$ Variables: $P, \sigma, \epsilon_1, \epsilon_2$ $\rho, \delta, \psi$ are constants defined in [54].	$\dot{\hat{x}} = A\hat{x} + B_u u + \phi(\hat{x}, u)$ $-L(y - \hat{y})$ $\hat{y} = C\hat{x} + D_u u$ $L = \frac{1}{2}\sigma P^{-1}C^\top$	find $\{\sigma, \epsilon_1, \epsilon_2\} > 0$ s.t. $\begin{bmatrix} A^\top P + PA + \epsilon_1 \rho I \\ + \epsilon_2 \delta I - \sigma C^\top C & P + \frac{\psi \epsilon_2 - \epsilon_1}{2} I \\ \left(P + \frac{\psi \epsilon_2 - \epsilon_1}{2} I\right)^\top & -\epsilon_2 I \end{bmatrix} \preceq O$
$\dot{x} = Ax + B_u u + \phi(x)$ $y = Cx + D_u u$ Variables: $P, Y, \kappa$ $\beta$ is the Lipschitz constant [55].	$\dot{\hat{x}} = A\hat{x} + B_u u + \phi(\hat{x})$ $-L(y - \hat{y})$ $\hat{y} = C\hat{x} + D_u u$ $L = P^{-1}Y$	find $Y, \kappa > 0$ s.t. $\begin{bmatrix} A^\top P + PA - YC \\ -C^\top Y^\top + 2\alpha P + \kappa \beta^2 I & P \\ P & -\kappa I \end{bmatrix} \preceq O$